Oxygen, Carbon and pH Variability in the Indian Ocean

Raleigh R Hood, Tim Rixen, Marina Levy, Dennis A Hansell, Victoria J Coles, Zouhair Lachkar

Oxygen, Carbon and pH Variability in the Indian Ocean

Raleigh R. Hood, Horn Point Laboratory, University of Maryland Center for Environmental Science, Cambridge, MD, 21613, USA

Tim Rixen, Leibniz Centre for Tropical Marine Research, University of Bremen, Bremen, 28359, Germany

Marina Levy, LOCEAN-IPSL, Sorbonne University, 75252 Paris Cedex O5, France

Dennis A. Hansell, Rosenstiel School of Marine and Atmospheric Science, University of Miami, 4600 Rickenbacker Causeway, Miami, FL 33149, USA

Victoria J. Coles, Horn Point Laboratory, University of Maryland Center for Environmental Science, Cambridge, MD, 21613, USA

Zouhair Lachkar, Center for Prototype Climate Modeling, New York University, Abu Dhabi, PO Box 129188, Saadiyat Island, Abu Dhabi, United Arab Emirates

Abstract

This chapter provides an overview of the physical and biogeochemical factors that control spatial and temporal patterns of oxygen minimum zones (OMZs), carbon and pH variability in the Indian Ocean. Oxygen concentrations decline to nearly zero in Arabian Sea intermediate water with profound biogeochemical impacts on the nitrogen cycle as a result of denitrification. These impacts can hardly be observed in the Bay of Bengal where oxygen concentrations are poised just above the threshold below which denitrification becomes significant. Hypoxic/anoxic conditions in the open ocean waters of the northern Indian Ocean have not dramatically changed over past decades, but evidence is now emerging that oxygen concentrations are starting to decline, with significant biogeochemical and ecological impacts. The Indian Ocean accounts for ~1/5 of the global oceanic uptake of atmospheric CO_2, with the Arabian Sea as a source of CO_2 to the atmosphere and the southern subtropical gyre as a CO_2 sink. Net CO_2 flux in the Bay of Bengal is uncertain due to sparse sampling. Surface pH values in the Indian Ocean are anomalously low and projected to decline further with negative impacts on calcifying organisms. Dissolved organic carbon (DOC) concentrations in the Indian Ocean tend to be high in near-surface (sub)tropical waters where autotrophic production of DOC exceeds heterotrophic consumption and vertical stability of the water column favors accumulation. In contrast, the highest particulate organic carbon (POC) concentrations in the Indian Ocean are observed in the northwestern part of the basin and the lowest in the southern subtropical gyre, reflecting primary production patterns. POC export flux patterns in the Indian Ocean are similar to the patterns in POC concentration, though carbon flux is also strongly influenced by lithogenic matter content in river-influenced regions like the Bay of Bengal. Observational and modeling research should target improved understanding of northern Indian Ocean OMZ and carbon system variability as such is needed to predict the impacts of anthropogenic influence and global warming on Indian Ocean biogeochemistry and ecosystems.

1. Introduction

1.1 The Northern Indian Ocean oxygen minimum zones (OMZs)

Open ocean Oxygen Minimum Zones (OMZs) occur below the mixed layer of the ocean and are characterized by oxygen concentrations that are low in comparison to surface and deep waters (Dietrich, 1936; Seiwell, 1937; Sverdrup, 1938). Even though mid-water oxygen minimum zones are common features in the ocean, they are typically classified as OMZs only when the lowest minimum oxygen concentrations in the vertical profile drop below certain thresholds (Paulmier et al., 2009). However, due to varying oxygen tolerances of marine organisms, there are multiple definitions for threshold concentrations. Table 1 lays out common definitions, thresholds and impacts of varying definitions of oxygen limitations. A threshold of about 20 µmol/kg is often used to define OMZs because concentrations below this have profound implications for microbes and marine biogeochemical cycles. These oxygen levels are therefore referred to as "microbial hypoxia" (Table 1). The total volume of waters characterized by microbial hypoxia in the global ocean is approximately 15 x 10^{15} m^3, of which 21% (3.13 x 10^{15} m^3) is located in the northern Indian Ocean (Acharya et al., 2016; Garcia et al., 2010). Even though the Indian Ocean OMZ constitutes only 0.23% of the ocean's volume (1355 x 10^{15} m^3) its influence on the cycles of nitrogen, carbon and associated elements is globally significant.

The thickest OMZ in the world is found in the Arabian Sea (e.g., Morrison et al., 1999) where functional anoxia (concentrations < .05 µmol/kg, Table 1) occurs in intermediate water (~200-800 m), with profound impact on the nitrogen cycle as a result of denitrification. Very low oxygen concentrations are also found in intermediate water in the Bay of Bengal, but there are important physical and biogeochemical differences between the Arabian Sea and the Bay of Bengal, which have, so far, prevented the development of persistent functional anoxia in the Bay of Bengal OMZ (Figures 1 and 2). Hence in contrast to the Bay of Bengal, the Arabian Sea OMZ is a globally important zone of denitrification (Naqvi et al., 2005), where NO_3^- and NO_2^- are converted to N_2O and N_2 gas, which is then released to the atmosphere. This process of denitrification removes nitrogen containing compounds from the ocean (Figures 1 and 2) and generates N_2O, a prominent greenhouse gas (Ramaswamy et al., 2001, Bange et al. 2001). The Arabian Sea OMZ is most intense in the eastern part of the basin (Figures 1 and 2), with the water column contributing ~10 - 20% of global open-ocean mid-water column denitrification (Codispoti et al., 2001; Rixen et al., 2020; Anju et al., 2022).

Questions remain regarding the relative roles of biological oxygen demand derived from surface organic matter export, versus circulation and ventilation timescales, in maintaining subtle differences in the deep oxygen fields in the Arabian Sea and the Bay of Bengal (Valsala et al., 2009; McCreary et al., 2013; Bopp et al., 2017; Rixen et al., 2020). Recent observational and modeling studies in the Indian Ocean suggest that the OMZs are expanding in response to global warming (Lachkar et al., 2020; Rixen et al., 2020). Perhaps the low nitrogen to phosphorus ratios in the western Bay of Bengal are a harbinger of what is to come (Figure 1). This OMZ expansion is consistent with global modeling studies (Stramma et al., 2008; 2010; Doney, 2010; Figure 3) but uncertainties in global model predictions are large (McCreary et al., 2013; Bopp et al., 2017; Rixen et al., 2020; Kwiatkowski et al., 2020; Schmidt et al., 2020; Schmidt et al., 2021).

Given the importance of the Indian Ocean OMZs in the global carbon and nitrogen cycles, including the production of radiatively active greenhouse gas, it is essential to understand the biogeochemical variability associated with these regions, their rates of change and the potential implications for global warming.

1.2 Role of the Indian Ocean in the global carbon cycle

The Indian Ocean plays an important role in the global carbon cycle, yet it remains one of the most poorly sampled ocean regions with respect to inorganic and organic carbon pools and air-sea carbon fluxes (Figures 4, 5 and 6). Estimates suggest that the Indian Ocean accounts for a significant fraction of the global oceanic uptake of atmospheric CO_2 (Takahashi et al., 2002; Sarma et al., 2013; Valsala and Maksyutov, 2013; Sreeush et al., 2018; 2020; de Verneil et al., 2021). This uptake of anthropogenic CO_2 drives a decrease in pH, and indeed, surface pH values in the Indian Ocean are among the lowest of the major ocean basins (Feely et al., 2009; Sreeush et al., 2019). Projected increases in oceanic CO_2 concentrations will lead to further acidification of the Indian Ocean over the coming decades, with potentially severe negative impacts on coral reefs and other calcifying organisms (Hoegh-Guldberg et al., 2007; Doney, 2010).

Dissolved organic carbon (DOC) is a significant carbon pool in the ocean. As observed elsewhere in the global ocean, DOC concentrations in the Indian Ocean tend to be high in stratified near-surface tropical and subtropical waters where DOC is produced and accumulates, and DOC concentrations are lowest in the deep ocean where heterotrophic consumption of DOC exceeds autotrophic production (Hansell, 2009; Hansell, et al., 2009; Figures 6 and 7). Unsurprisingly, the highest concentrations of DOC are found in the near-surface waters of the central Arabian Sea due to high autotrophic production, and in the northern Bay of Bengal due to the large inputs of fresh water and associated terrigenous DOC flux from rivers (Hansell, 2009; Shah et al., 2018; Figure 6; Data from Hansell and Orellana, 2021). In contrast, particulate organic carbon (POC) concentrations tend to be high in coastal regions of the Indian Ocean where autotrophic production is high, and lowest in the oligotrophic southern subtropical gyre and equatorial waters where autotrophic production is low (Gardner et al., 2006; Figure 8). The highest POC concentrations are found in the western and northern Arabian Sea during the southwest monsoon (SWM) and northeast monsoon (NEM), respectively (Gardner et al., 2006). The spatial and temporal variability in POC export flux in the Indian Ocean is similar to the productivity and POC concentration patterns, consistent with the idea that primary productivity is the main control on the spatial and temporal variability of organic carbon fluxes (Rixen et al., 2019a). However, in regions strongly influenced by river inputs, like the Bay of Bengal, the spatial variability of organic carbon export flux is also strongly influenced by lithogenic matter content, which provides ballast that increases POC sinking rates (Rixen et al., 2019b).

Understanding and predicting these disparate elements of the carbon cycle and its role in basin acidification in the Indian Ocean is critical for understanding the biogeochemical and ecological evolution of the Indian Ocean under the impact of human activities.

2. Oxygen concentrations and the biogeochemical impacts of the OMZs

The first large ocean-going oceanographic expeditions discovered OMZs in the Indian Ocean between the end of the 19th and the first third of the 20th century (Sewell, 1934; Sewell and Fage, 1948 and references therein). During one of these cruises, the John Murray expedition of 1933 – 34, Gilson (1933) discovered the secondary nitrite maximum of the Arabian Sea, seen as an accumulation of nitrite within the upper part of the OMZ between 200 and 300m depth (Figure 2). Its existence indicates active denitrification (Naqvi, 1991), which in addition to anammox (Dalsgaard et al., 2003; Kuypers et al., 2003) are the main sinks of fixed nitrogen (NH_4^+, NO_2^-, NO_3^-) in the ocean (Gruber, 2004). Denitrifying microbes use nitrate (NO_3^-) and nitrite (NO_2^-) to fuel heterotrophic respiration in microbially hypoxic waters, in turn reducing these compounds, ultimately, to nitrogen gas (N_2). In contrast, the annamox reaction is carried out by chemoautotrophic microbes that derive energy from the oxidation of NH_4^+ with NO_2^- to produce N_2 in microbially hypoxic waters.

In contrast to fixed nitrogen, N_2 is inaccessible to eukaryotic phytoplankton. Even though there are specific bacterial phytoplankton clades capable of fixing or breaking apart and oxidizing N_2, the surface ocean is often depleted in fixed nitrogen in comparison to phosphate (Gruber and Sarmiento, 1997). Since phosphate and fixed nitrogen are the primary macro-nutrients required for phytoplankton growth, the intensification of OMZs and the expansion of functional anoxia is assumed to lower marine productivity by favoring denitrification and anammox and thereby the loss of fixed nitrogen in the ocean (Altabet et al., 1995; McElroy, 1983). An interesting feedback is that, over time, reduced productivity and carbon export due to fixed nitrogen loss in turn reduces biological oxygen consumption at depth, such that the expansion of the volume of anoxic waters in the OMZ core can be accompanied by a reduction of the volume of hypoxic waters (Deutsch et al., 2007; Lachkar et al., 2016).

Changes in the coupled marine nitrogen and oxygen cycles also affect the role of the ocean as a sink and/or source of greenhouse gases such as CO_2 and N_2O. The response of the biologically mediated CO_2 uptake of the ocean, referred to as the biological carbon pump (Boyd et al., 2019; Volk and Hoffert, 1985), to environmental changes is difficult to predict (Bopp et al, 2013, De La Rocha and Passow, 2014) because of the multiple processes involved in its functioning (Chakraborty et al., 2018; Boyd et al., 2019). In contrast, the N_2O source function of the ocean is assumed to be directly linked to the expansion and intensity of OMZs, since N_2O is an intermediate product formed during denitrification (Bange et al., 2001; Fuhrman and Capone, 1991).

Even though denitrification and anammox occur at microbially hypoxic levels of oxygen (concentrations < 20 μmol/kg; Table 1), their impact on the nitrogen cycle becomes significant only with the occurrence of functional anoxia (concentrations < .05 μmol/kg; Table 1). At such low oxygen concentrations, the reduction of nitrite to N_2 outcompetes the re-oxidation of nitrite to nitrate, leading to net loss of fixed nitrogen (Bristow et al., 2017; Gaye et al., 2013). The re-oxidation of nitrite to nitrate prevents, in turn, the loss of fixed nitrogen and the formation of the secondary nitrite maximum at higher oxygen concentrations within the OMZ. In contrast to the Bay of Bengal OMZ, which is on the verge of becoming functionally anoxic (Bristow et al., 2017), functional anoxia is wide spread in the Arabian Sea OMZ as indicated by the extent of the secondary nitrate maximum (Naqvi, 1991; Rixen et al., 2014; Figure 2).

2.1 Oxygen distributions, sources and sinks

Low oxygen conditions in the water column are usually associated with slow ventilation and high biological oxygen demand. OMZs are hence found in productive but poorly ventilated shadow zones of the subtropical oceans, where subsurface water masses recirculate beneath a shallow mixed-layer with minimal direct advective or mixing connection to the surface ocean (Luyten et al., 1983). In these domains, the residence time below the thermocline is at a maximum and oxygen is slowly supplied mainly through isopycnal (horizontal) mixing processes (Gnanadesikan et al., 2012; Levy et al., 2021). Moreover, the strong and localized subsurface biological oxygen consumption in OMZs generates strong spatial gradients in oxygen at their edges, making mixing central to the oxygen balance. The Arabian Sea OMZ is not a classical shadow zone due to the northern boundary of the Asian subcontinent, but diapycnal and isopycnal mixing are likely the main oxygen sources balancing strong biological depletion in the core of the OMZ, in roughly equal proportions (Resplandy et al., 2012). Model simulations suggest that without oxygen supplied by eddy mixing, the volume of the Arabian Sea OMZ would double (Lachkar et al., 2016).

In addition to mixing processes in the core of the OMZ, the inflow of oxygen-enriched Indian Ocean Central Water and Persian Gulf Water are assumed to be the main physical oxygen supply mechanism to the edges of the OMZ in the Arabian Sea (Lachkar et al., 2019; McCreary et al., 2013; Resplandy et al., 2012; Sen Gupta and Naqvi, 1984; Swallow, 1984). Indian Ocean Central Water forms through convective mixing as Subantarctic Mode Water in the southern Indian Ocean and is advected northward into the OMZs in both the Arabian Sea and Bay of Bengal (Fine, 1993; McCartney, 1979; Sverdrup et al., 1942). Oxygen-enriched Persian Gulf Water is introduced into the Arabian Sea OMZ after its outflow from the Persian Gulf (Rixen et al., 2005; Schmidt et al., 2020; Schmidt et al., 2021; Tchernia, 1980; Lachkar et al. 2019). The negative water balance of the Persian Gulf drives this localized deep-water formation by increasing the salinity and hence the density of Persian Gulf Water.

The oxygen-poor Arabian Sea intermediate water, in turn, flows into the Bay of Bengal OMZ (Figure 1), where high freshwater inputs from rivers and monsoon rainfall (Figure 5) reduce the vertical oxygen supply by increasing stratification in the surface layers (Rixen et al., 2020). However, in comparison to the Arabian Sea, lower biomass (Figure 8), productivity and a stronger ballast effect prevent development of functional anoxia in the Bay of Bengal OMZ by keeping biological oxygen consumption lower (Al Azhar et al., 2017; Rao et al., 1994; Rixen et al., 2019b). Ballast minerals, which are supplied from land via rivers or as dust, accelerate the sinking of particles, lowering the residence time of exported organic matter in the water column and thereby its decomposition in the OMZ (Haake and Ittekkot, 1990; Ramaswamy et al., 1991). It should be noted, however, that the ballast effect appears to be important primarily in the northern Bay of Bengal (Ittekot et al., 1991), which suggests that the primary cause of the higher oxygen concentrations further south in the Bay of Bengal is the lower biomass and productivity that results in reduced export and a lower biological oxygen demand. In contrast to the Bay of Bengal, a weak ballast effect and a higher biological production (Figure 8) sustain a higher biological oxygen consumption at intermediate depths in the Arabian Sea. This enhanced biological oxygen consumption balances the higher physical oxygen supply in the Arabian Sea and explains the more intense OMZ (Rixen et al., 2019a).

Contrary to expectations, the Arabian Sea OMZ is more intense in the eastern part of the basin and less intense in the western parts of the basin where productivity is highest (Antoine and Morel, 1996; Naqvi, 1991; McCreary et al., 2013). The thickest part of the OMZ is in the northeastern Arabian Sea (Sarma et al., 2020). Multiple factors are presumed to cause this asymmetry. The inflow of Indian Ocean Central Water and Persian Gulf Water ventilates the western Arabian Sea preferentially, and is assumed to cause this eastward displacement (Resplandy et al., 2012; McCreary et al., 2013; Rixen et al., 2014). Additionally, the seasonal monsoon-driven reversal of the surface ocean circulation leads to intense vertical eddy mixing in the western Arabian Sea causing an eastward shift of the upper OMZ relative to the region of highest productivity (Resplandy et al., 2012; McCreary et al, 2013; Lachkar er al., 2016). Similarly, the eastward shift of the OMZ has been attributed to weak mixing and high penetration time of intermediate water masses in the northeastern Arabian Sea, with the additional influence of organic matter transport from the shelf region that enhances biological oxygen demand (Sarma et al., 2020).

2.2 Biogeochemical impacts of the northern Indian Ocean OMZs

The Arabian Sea and the Bay of Bengal collectively contain ~59% of the Earth's marine sediments exposed to hypoxia (Helly and Levin, 2004). Denitrification within sediments (benthic denitrification) underlying functionally anoxic conditions in the water column, is the largest sink for fixed nitrogen in the ocean (Gruber, 2004; DeVries et al., 2013). However, estimates of the relative rates of benthic and water column denitrification are still fraught with large uncertainties on global as well as regional scales. Hence, the role of the Arabian Sea as a sink of fixed nitrogen is difficult to quantify. Although denitrification in the Arabian Sea has been much more intensively studied than in the Bay of Bengal, estimates of benthic and water column denitrification in the Arabian Sea still encompass a wide range with means of 3.9 ± 2.9 Tg N $year^{-1}$ and 17 ± 16 Tg N $year^{-1}$, respectively (Bange et al., 2000; Bristow et al., 2017; Deuser et al., 1978; Gaye et al., 2013; Howell et al., 1997; Naqvi et al., 1982; Somasundar et al., 1990). Considering global mean estimates of benthic and water-column denitrification of 183 ± 118 Tg N $year^{-1}$ and 155 ± 116 Tg N $year^{-1}$ (Eugster and Gruber, 2012; Gruber, 2004; Somes et al., 2013), on average the Arabian Sea comprises approximately 2% and 11% of the global mean benthic and water column denitrification, respectively. It should be noted, however, that more recent data indicate that benthic denitrification at the Pakistan continental margin alone could be up to 10.5 Tg N $year^{-1}$ (Schwartz et al., 2009; Somes et al., 2013), greatly exceeding the previously estimated benthic denitrification of 3.9 ± 2.9 Tg N $year^{-1}$ for the entire Arabian Sea. Moreover, the most recent observations suggest the northeastern Arabian Sea has a water column denitrification rate of 25.3 ± 7.0 Tg N yr^{-1} (Anju et al., 2022). These estimates suggest that the Arabian Sea comprises at least 6% and 16% of the global mean benthic and water column denitrification, respectively.

The volume of hypoxic waters and rate of denitrification in the Arabian Sea strongly increase in response to enhanced monsoon winds (Lachkar et al., 2018). Stronger winds intensify the upwelling, increasing biological productivity and respiration in excess of the increase in wind-driven ventilation and are also responsible for the deepening of the OMZ. However, as discussed above, increases in denitrification have the potential to reduce biological productivity through nitrogen removal, and hence the efficiency of the biological pump of carbon, at the basin scale (and beyond) on timescales of decades to centuries (Lachkar et al., 2018; Canfield et al., 2019; McElroy, 1983). Therefore, an expansion of Indian Ocean OMZs can affect the large-scale biogeochemical cycles of nitrogen and carbon and contribute to climate variations over long timescales (Altabet et al., 2002; Gaye et al., 2018). The extent of this control depends on the magnitude of the nitrogen removal and the importance of concurrent stabilizing negative feedbacks, including the feedback of reduced productivity on biological oxygen demand and the tight coupling between denitrification and N_2 fixation downstream of OMZs (Deutsch et al., 2007, Gruber and Galloway, 2008). If the excess in phosphorus relative to nitrogen supports local nitrogen fixation within the Indian Ocean basin, the timescales for feedbacks with denitrification could be much shorter than the timescale of the global ocean circulation.

2.3 Recent (decadal) changes in oxygen concentrations

Early reports on the occurrence of coastal hydrogen sulfide in the north-eastern Arabian Sea and off Oman at Ras-al-Hadd (Carruthers et al., 1959; Ivanenkov and Rozanov, 1966) indicate that the Arabian Sea OMZ was more intense in the past because the emergence of hydrogen sulfide indicates the transition from functional anoxia (oxygen < .05 μmol/kg) towards anoxic (zero oxygen) conditions (Table 1). These are the only reports of the occurrence of hydrogen sulfide in the Arabian Sea except for Naqvi et al. (2000), who discovered an anoxic event that developed along the western Indian coast off Mumbai in the late summer of 1999. Such strong events do not develop every year (Gupta et al., 2016; Sudheesh et al., 2016), but their appearance shows that the spreading of oxygen-depleted zones in coastal regions is a global phenomenon that does not spare the Indian shelf (Altieri et al., 2017; Diaz and Rosenberg, 2008; Diaz et al., 2019). However, contrary to this prevailing understanding, Gupta et al. (2021) argue that the hypoxic-anoxic zone along the west coast of India is formed through a natural process, i.e., upwelling of deoxygenated waters during the summer monsoon, and that the persistence and extent of this coastal oxygen deficiency depend on the degree of deoxygenation of source waters for the upwelling. Moreover, the volume of anoxic waters is strongly modulated by the Indian Ocean Dipole (IOD), with positive IOD events preventing anoxia due to wind-forced downwelling coastal Kelvin waves propagating along the west coast of India (Vallivattathillam et al., 2017).

In contrast to these shelf processes, there is only a weak decadal decline in dissolved oxygen concentrations in the OMZs of the Arabian Sea and the Bay of Bengal in comparison to OMZs of the South Atlantic Ocean and the Pacific Ocean (Ito et al., 2017; Naqvi, 2019; Schmidtko et al., 2017; Stramma et al., 2008). The analysis of all oxygen data available from the Arabian Sea between 1959 and 2004 by Banse et al. (2014) ascribes this modest change to opposing regional trends within the Arabian Sea, where oxygen concentrations increased in the southern part of the Arabian Sea and declined in the central Arabian Sea. In contrast, Sarma et al. (2018) ascribe the modest change in oxygen levels in the Bay of Bengal to the influence of anticyclonic eddies in that precluded the OMZ from intensifying. Follow-up studies report decreasing oxygen concentrations in the western and northern Arabian Sea (Piontkovski and Al-Oufi, 2015; Queste et al., 2018). In the northern Arabian Sea, dissolved oxygen concentrations in the surface mixed layer largely reflect the decreasing trend seen in the OMZ, as indicated by a compilation of dissolved oxygen data covering the period from the 1960s to 2010 (Gomes et al., 2014). In response to this deoxygenation, the secondary nitrite maximum expanded southward and westward in the early 1990s (Rixen et al., 2014). Perhaps in response to changing oxygen concentrations, the planktonic community structure has changed as shown by the development and now regular occurrence of large *Noctiluca* winter blooms since the 2000s in the Arabian Sea (Hood et al, 2022 this volume; Gomes et al, 2014; Goes and Gomes, 2016; Goes et al., 2020). It should be noted, however, that it has been shown that *Noctiluca* blooms occur in oxic conditions, and that both natural and anthropogenic processes appear to have contributed to the development of the massive blooms in the northeastern Arabian Sea (Sarma et al., 2018; Sridevi and Sarma, 2022). Numerical model results suggest that reduced ventilation caused by a reduced inflow of Persian Gulf Water in response to warming, combined with reduced solubility of oxygen in surface water of the Persian Gulf, may have contributed to these developments (Lachkar et al., 2019). In addition to changes in the Gulf outflow, recent numerical model results also attribute decreasing oxygen concentrations in the northern Arabian Sea to reduced local ventilation due to global warming-induced increases in stratification and weakening of winter convective mixing (Lachkar et al., 2020).

Nonetheless, widespread and or more frequent outbreaks of hydrogen sulfide as seen in the upwelling systems off Peru (Schunck et al., 2013) and Namibia (Weeks et al., 2002) have not so far been reported in the northern Indian Ocean during the last 50 years. This finding implies that the interplay between physical oxygen supply and the biological oxygen consumption has prevented the development of persistent anoxia (zero oxygen) in the Arabian Sea and functional anoxia (oxygen $< .05$ μM) in the Bay of Bengal OMZ (Rixen et al., 2020).

2.4 Future changes in oxygen concentrations

There is high uncertainty in the future evolution of the Arabian Sea OMZ, and of all major OMZs, projected by Earth System models by year 2100 (Bopp et al., 2013, Cabré et al. 2015, Kwiatkowski et al., 2020; Rixen et al., 2020). The uncertainty largely arises from differences among models in the magnitude and timing of changes in ventilation and biological oxygen demand and how strongly they offset each other (Resplandy, 2018). Both processes are strongly influenced by model resolution and are thus challenging to simulate at the centennial scale. It is projected that OMZs may either shrink or expand under projected climate change, depending on the efficiency of mixing (Duteil and Oschlies, 2011, Bahl et al., 2019, Lévy et al., 2021). As discussed above, this uncertainty is particularly large in the northern Indian Ocean where global forecast models generally fail to reproduce the current oxygen concentrations and distributions (McCreary et al., 2013; Rixen et al., 2020; Schimdt et al., 2021). This failure, and the uncertainty in future projections, may also be related to the lack of consideration of the role of cross-shelf transport of organic matter in Earth System models, which is a process that is known to contribute to the development of the OMZs in both the Arabian Sea and Bay of Bengal (Sarma et al., 2020; Udaya Bhaskar et al., 2021).

3. Carbon concentrations and fluxes

The earliest CO_2, pH and POC measurements in the Indian Ocean date back to the International Indian Ocean Expedition in the early1960s (Figure 4; e.g., Newell, 1969; Berhman, 1981). Carbonate system measurements were also made in the Indian Ocean under the Geochemical Ocean Section Study (GEOSECS) in the 1970s (Moore, 1984), the Joint Global Ocean Flux Study (JGOFS; Fasham, 2003; see also https://en.wikipedia.org/wiki/Joint_Global_Ocean_Flux_Study) and the World Ocean Circulation Experiment (WOCE) in the 1990s (Woods, 1985). Subsequently in the first decade of the 21st century CLIVAR Repeat Hydrography project started (Gould et al., 2013), and carbonate system measurements continue through the present under the ongoing GO-SHIP program (Talley et al, 2017; see also https://www.go-ship.org/About.html) and the Second International Indian Ocean Expedition (IIOE-2; Hood et al., 2015). In addition to these major international efforts, there have been numerous national expeditions and programs that have contributed to the current inventory of carbonate system measurements in the Indian Ocean. For example, time-series observations of pH and pCO_2 are being made in the coastal waters of India revealing recent trends (Sarma et al., 2021). There is also now a mooring in the central Bay of Bengal (Figure 4) that has been collecting continuous CO_2 and pH measurements since November, 2013 (see https://www.pmel.noxsaa.gov/co2/story/BOBOA).

In contrast, the history of DOC measurements in the Indian Ocean dates back only to the early 1990s when it was discovered (thanks to advances in measurement methods that achieved ~ 1 μmol/kg precision sufficient to reveal DOC variability over space and time) that DOC concentrations are more dynamic than previously thought (Hansell, 2009). The timing of this discovery coincided with the onset of the JGOFS Arabian Sea Process Study when some of the earliest "modern" Indian Ocean DOC measurements were made. Subsequently, DOC concentration measurements were made in the Indian Ocean under the US CLIVAR Repeat Hydrography project and they continue under the ongoing GO-SHIP program and through national expeditions. DOC isotopes measurements are also now being made in the northern Indian Ocean to provide insight into DOC sources (Rao and Sarma, 2022).

3.1 Inorganic carbon distributions and fluxes

The Indian Ocean accounts for ~20% of the global oceanic uptake of atmospheric CO_2 (Takahashi et al., 2002). The Arabian Sea is a source of CO_2 to the atmosphere due to elevated pCO_2 within the Southwest Monsoon (SWM)-driven upwelling (Figure 4; see also Takahashi et al., 2009; 2014; Valsala and Maksyutov, 2010; 2013; de Verneil et al., 2021). North of 14°S the Indian Ocean loses CO_2 at a rate of 0.12 – 0.16 PgC/yr (Takahashi et al., 2002; 2009; 2014; de Verneil et al., 2021). The most intense air-sea CO_2 exchange occurs during the SWM where outgassing rates reach ~6 molC/m^2/yr in the upwelling regions off Oman and Somalia, but the entire Arabian Sea contributes CO_2 to the atmosphere (Valsala and Murtugudde, 2015; Sreeush et al., 2018; 2020; de Verneil et al., 2021).

Time series measurements have shown that the rates of increase in DIC and pCO_2 per decade are consistent with global trends in the southwestern coastal Bay of Bengal, whereas rates in the northwestern coastal Bay of Bengal have been observed to be 3 to 5 times higher than the global trends (Sarma et al., 2015a). Thus, the northwestern Bay of Bengal, which was previously considered to be a significant sink for atmospheric CO_2, now seems to have become a source of CO_2 to the atmosphere. Variability in CO_2 fluxes in the northwestern shelf region of the Bay of Bengal depends on the river discharge characteristics and the East India Coastal Current that distributes this water along the coast (Sarma et al., 2012). Nonetheless, it is still uncertain whether the entire Bay of Bengal is a net CO_2 source or sink due to the high levels of variability combined with sparse spatial and temporal sampling (Figure 4; Bates et al., 2006). South of 14°S the Indian Ocean appears to be a strong net CO_2 sink (-0.44 PgC/yr in the band 14°S-50°S; Figure 4). The solubility pump (CO_2 dissolution and its physical mixing and transport) and the biological pump (biologically mediated processes that export carbon) contribute equally to the CO_2 sink in the south Indian Ocean region (Valsala et al., 2012). Cold temperatures increase CO_2 solubility at higher latitudes and subduction in the subtropical front can transport this CO_2 into the ocean interior, but there is also evidence that chemical and biological factors are important, e.g., potential iron fertilization that facilitates particulate carbon export in the southern hemisphere of the Indian Ocean (Piketh et al., 2000).

In addition, the IOD leads to a substantial sea-to-air CO_2 flux variability in the southeastern tropical Indian Ocean over a broad region (70–105°E, 0–20°S), with the most intense effects manifesting near the coast of Java-Sumatra due to the impacts on upwelling dynamics and associated westward propagating anomalies. The sea-to-air CO_2 fluxes, surface ocean partial pressure of CO_2 (pCO_2), the concentration of dissolved inorganic carbon (DIC), and ocean alkalinity (ALK) range as much as ±1.0 mole m^{-2} yr^{-1}, ±20 µatm, ±35 µmole kg^{-1}, and ±22 µmole kg^{-1}, respectively, within 80–105°E, 0–10°S due to the IOD. The DIC and ALK are significant drivers of pCO_2 variability associated with IOD (Valsala et al., 2020).

Synthesis of the seasonal, annual and interannual air-sea CO_2 fluxes based on both models (ocean, atmospheric inversions) and observations (Takahashi et al., 2009) reveals that the net sea-air CO_2 uptake estimated from observations (-0.24 PgC/yr) is consistent with uptake derived from models (-0.37 PgC/yr), given the uncertainties (Sarma et al., 2013). However, some models overestimate flux in the Bay of Bengal and underestimate flux in the Arabian Sea / northwestern Indian Ocean (Sarma et al., 2013). These offsets are likely due to the models being inadequately constrained by CO_2 observations. There are fewer observations in the Indian Ocean (especially north of 20ºS) compared to other oceans in recent years (Figure 4; Bakker et al., 2014, see also www.socat.info). More observations of ocean DIC concentrations and carbon flux are needed in the Indian Ocean to constrain the models and reduce uncertainties in the fluxes. Toward this goal, Valsala et al. (2021) has recently done observing system simulation experiments for Indian Ocean pCO_2 arrays and recommended deployment of additional moorings at suitable locations to monitor and better constrain the Indian Ocean air-sea CO_2 fluxes. A few key ship-of-opportunity routes for underway pCO_2 sampling in the Indian Ocean are also recommended in their study.

3.2 Spatial and temporal variability in pH

Uptake of anthropogenic CO_2 by the ocean results in fundamental changes in seawater chemistry that can have significant impacts on ocean ecosystems (Doney et al., 2010; Gattuso and Hansson, 2011). Intergovernmental Panel on Climate Change (IPCC) business-as-usual emission scenarios indicate that atmospheric CO_2 levels will reach 800 ppm near the end of this century (Feely et al., 2009). The associated increase in oceanic CO_2 concentrations will lead to acidification (lower pH) of the Indian Ocean over the coming decades, with potential severe negative impacts on coral reefs and other calcifying organisms (Doney, 2010; IPCC, 2019). In 1995, the surface pH values for the northern (20°E-120°E, 0°-24.5°N) and southern (20°E-120°E, 0°-40°S) Indian Oceans were 8.068 +/- 0.03 and 8.092 +/- 0.03, respectively, which is the lowest of the major ocean basins (Feely et al., 2009). It is not entirely clear why surface pH values are so low in the Indian Ocean (Takahashi et al., 2014). Increases in sulphate and nitrogen aerosol loadings over the Bay of Bengal from the Indo-Gangetic Plain and Southeast Asia may be mainly responsible for the increased acidity in the northwestern Bay of Bengal in recent years (Sarma et al., 2015a). Reduced Godavari River discharge together with a positive IOD event have also been shown to contribute to enhanced acidification and pCO_2 levels in the coastal waters in the western Bay of Bengal (Sarma et al., 2015b). A study from the eastern Bay of Bengal indicates a decline in pH of 0.2 from 1994 to 2012 (Rashid et al., 2013), which is considerably faster than the global decline of 0.1 over the last century (IPCC 2007). Upwelling of low pH subsurface waters in the Arabian Sea results in low surface pH (<7.9) during the SWM (Takahashi et al., 2014). Sreeush et al. (2019) estimated that in addition to the anthropogenic causes, ocean warming exacerbates acidification in the western Arabian Sea by an additional 16%. Chakraborty et al. (2021) studied the seasonal drivers of surface ocean pH in the Arabian Sea and Bay of Bengal and found that DIC and SST make complementary contributions to the seasonal cycle in pH. Tarique et al. (2021) reported the first time series of Arabian Sea pH from proxy records of Boron Isotopes from 1990 to 2013. Their investigation reveals that physical oceanographic processes, for example, upwelling, downwelling and convective mixing modulated by El Niño-Southern Oscillation (ENSO), largely control surface pH variability and mask expected long-term ocean acidification trends resulting from anthropogenic CO_2 rise. An increase in pH has been observed in the eastern and southern Bay of Bengal during all seasons associated with warming and a decrease in salinity (Sridevi and Sarma, 2021). In contrast, a decrease in pH (-0.001 yr^{-1}) and a pCO_2 increase (+0.1 to +0.7 µatm yr^{-1}) has been observed in the western and northern Bay of Bengal during winter and spring seasons due to deposition of atmospheric pollutants (Sridevi and Sarma, 2021). These studies suggests that increases in freshwater input due to melting of Himalayan ice cover and deposition of atmospheric pollutants are dominant controlling factors on surface ocean pH and pCO_2 in the Bay of Bengal between 1998 and 2015, and this region is acting as a stronger sink for the atmospheric CO_2 in the present than in the past two decades (Sarma et al., 2021; Sridevi and Sarma, 2021).

The susceptibility of the Indian Ocean coral communities to warming has been revealed by the large-scale coral bleaching events of 1998, 2005, 2011 as well as between 2014 and 2017 caused by high SST (McClanahan et al., 2007; Moore et al., 2012, Obura et al. 2017, Cerutti et al. 2020). Ocean acidification has the potential to exacerbate these negative impacts on coral reef ecosystems. For example, the 1998 bleaching event altered the age distribution of commercially harvested fish (Graham et al. 2007). Because of the combined effects of acidification, human development and global warming, coral reef ecosystems may be at greater risk than previously thought (Hoegh-Guldberg et al., 2007; IPCC, 2019). Moreover, some commercially fished species (e.g., shelled mollusks) are directly vulnerable to ocean acidification (Hoegh-Guldberg et al., 2014). A study off Somalia suggests that human-induced ocean acidification reduced the rate at which foraminifera calcify, resulting in lighter shells (de Moel et al., 2009). Due to the effects of acidification on calcifying pteropods, which are preyed on by many higher trophic level organisms, the Southern Ocean sector of the Indian Ocean could experience major disruptions in pelagic food webs (Bednarsek et al., 2012).

In addition to the direct impacts of acidification, increasing CO_2 in the upper ocean could lead to increased primary productivity for some species (e.g., diazotrophic cyanobacteria; Hutchins et al., 2007), altering rates of nitrogen fixation and therefore the biogeochemistry of particulate organic matter formation and remineralization. Declines in pH also shift the chemical equilibrium from ammonia (NH_3) to ammonium (NH_4^+), which could alter key biogeochemical processes such as nitrogen assimilation by phytoplankton and microbial nitrification (Gattuso and Hansson, 2011).

3.3 Large scale DOC and POC distribution and fluxes

Near-surface (< 50 meters) DOC concentrations in the Indian Ocean vary between ~50 and 80 µmolC/kg with the lowest values occurring south of 40° S (Hansell, 2009; Hansell et al., 2009; Figures 6, 7). In general, near-surface concentrations of DOC are positively correlated with temperature and, to a lesser extent, they are negatively correlated with nutrient concentrations. The positive correlation with temperature happens because warm, low-latitude waters tend to be more strongly stratified, and there is reduced vertical mixing. As a result, DOC concentrations increase in these waters even though there are low rates of net DOC production because the DOC is not mixed away (Hansell, 2009). As a result, near-surface DOC concentrations in the Indian Ocean tend to be highest (> 70 µmolC/kg) in tropical and subtropical waters (Hansell, 2009; Hansell et al., 2009; Figure 7). These patterns are also found in the Atlantic and Pacific (Hansell, 2009; Hansell et al., 2009).

Near-surface DOC concentrations tend to be inversely correlated with nitrate, silicate and phosphate concentrations because, when these nutrients are consumed, DOC is produced (Hansell, 2009). Thus, a negative correlation is also observed between DOC and nitrate and phosphate concentrations in the deep waters (> 500 meters) of the Indian Ocean where DOC concentrations decline to < 50 µmolC/kg (Figure 7) and nitrate and phosphate concentrations are substantially enriched. However, these correlations are not observed between DOC and silicate concentrations because in deep waters of the Indian Ocean there are large gradients in silicate that are associated with very little change in DOC (Hansell, 2009).

As in the Pacific and Atlantic, the lowest DOC concentrations in the Indian Ocean (40 - 42 µmol/kg at 3000 meters) are found below 1000 meters depth (Figure 7; Figure 2 in Hansell, et al., 2009). Global observations show that DOC concentrations below 1000 meters depth in the Indian Ocean are comparable to those in the Atlantic and significantly higher than deep DOC concentrations in the Pacific (< 40 µmolC/kg at 3000 meters; Hansell et al., 2009). DOC concentrations decline below the euphotic zone because heterotrophic consumption exceeds autotrophic production (Hansell et al., 2009). Presumably, a significant fraction of the DOC below 1000 meters in the Indian Ocean is very old (> 4000 years) and refractory (resistant to bacterial consumption) as has been shown to be the case in the Atlantic and Pacific (Bercovici et al., 2018).

As observed elsewhere in the global ocean, satellite-estimated near-surface POC concentrations are elevated in coastal regions of the Indian Ocean with values often exceeding 120 mgC/m^3 (= 10 µmolC/kg; Figure 8; Gardner et al., 2006). The highest POC concentrations in the Indian Ocean are observed in the northwestern part of the basin in the Arabian Sea and off of the coast of Somalia with values estimated to be greater than 96 mgC/m^3 (= 8 µmolC/kg) extending well into the open ocean during the NEM (Figure 8). These high POC values are associated with high chlorophyll concentrations, although chlorophyll itself only accounts for > .6% of the POC and presumably the remainder is cellular and detrital material (Gardner et al., 2006). Note that C:Chl ratios range from ~15-158 by weight (Sathyendrenath et al, 2009). Elevated POC concentrations (> 72 mgC/m^3 = 6 µmolC/kg) are also observed in the Indonesian Throughflow region (particularly during the Southeast Monsoon, SEM) and off of southern Africa over the Agulhas Bank, and in the Agulhas Current and its retroflection, again associated with high chlorophyll concentrations (> .4% of POC; Figure 8, Gardner et al., 2006). The lowest POC concentrations in the Indian Ocean are observed between 40° S and 10° N in the oligotrophic southern subtropical gyre and equatorial waters where primary production is very low (Gardner et al., 2006; Figure 8; see below).

Unsurprisingly, the spatial and temporal variability in POC export flux in the Indian Ocean is similar to the above mentioned patterns in POC and chlorophyll concentration, consistent with primary production as the main control on the spatial and temporal variability of organic carbon fluxes (Rixen et al., 2019a). However, as discussed above, in river-influenced regions like the Bay of Bengal, the spatial variability of organic carbon flux is also strongly influenced by lithogenic matter content. Rixen et al. (2019b) estimate that lithogenic matter content enhances organic carbon flux rates on average by 45% and by up to 62% in river-influenced regions of the Indian Ocean. This strong ballast effect explains why organic carbon fluxes are lower in the highly productive western Arabian Sea than they are in the relatively unproductive southern Java Sea. This explanation appears to be broadly consistent with the earlier global estimates of organic carbon burial and sediment accumulation rates calculated by Janke (1996; Figure 9), indicating that both are elevated in the coastal and northern regions of the Arabian Sea where rates of primary production are very high, but river influence is small. In contrast, both organic carbon burial and sediment accumulation rates are elevated over a much larger area in the Bay of Bengal where primary production is lower, but river influence is large (Janke, 1996; Figure 9).

3.4 Regional DOC and POC distributions and fluxes

3.4.1 Arabian Sea

DOC in the surface ocean is a short-term reservoir for carbon, expanding and contracting seasonally. In the Arabian Sea the highest near-surface (< 50 meters) DOC concentrations (80-100 µmolC/kg) are observed near the coast when upwelling is not active. During the SWM, upwelling results in lowered near-surface DOC concentrations along the western side of the basin, i.e., DOC concentrations increase seaward from <70 µmolC/kg near the coast to >80 µmolC/kg in the central Arabian Sea. In the open ocean, the highest surface DOC concentrations (80-95 µmolC/kg) are observed during the Northeast Monsoon (NEM) and they remain high through mid SWM. The lowest open ocean near-surface DOC concentrations (65-75 µmolC/kg) are observed during late SWM and during the Fall Intermonsoon (Hansell and Peltzer, 1998; Hansell, 2009).

The seasonal accumulation of DOC north of 15°N in the Arabian Sea happens mostly during the NEM, and it has been estimated to be equivalent to 6-8% of annual primary production and 80% of net community production. In contrast, net DOC production is very small during the SWM (Hansell and Peltzer, 1998).

In the vertical, DOC concentrations decrease to values of <55 μmolC/kg at the top of the OMZ (~100 meters). Vertical layering is also observed in DOC concentrations in the Arabian Sea and is associated with vertical layering of the water masses, with Persian Gulf Water producing a clear signal of elevated DOC. DOC concentrations below 500 meters are low (<50 μmolC/kg) and relatively uniform across the basin and there appears to be little impact of the OMZ on DOC concentrations (Hansell and Peltzer, 1998; Hansell, 2009).

Consistent with satellite estimates (Gardner et al., 2006), in situ measurements of near surface (0 - 150 meters) POC concentrations in the Arabian Sea are generally high near the coast of Oman and decrease offshore throughout the year with concentrations often exceeding 12.5 μmolC/kg (Gunderson et al., 1998; Figure 10). The spatial distributions are always patchy due to the influence of mesoscale eddies and jets. Seasonal variations in POC concentrations in the upper 150 m can be the same order of magnitude as basin-wide spatial variations and these concentrations are strongly influenced by nutrient availability and mixing (Gunderson et al., 1998). POC and chlorophyll concentrations are clearly correlated (Figures 10 and 11), indicating that variability in phytoplankton production drives much of the observed POC variations (Gunderson et al., 1998; Gardner et al., 2006). Subsurface POC and chlorophyll maxima are also observed, particularly offshore and during the intermonsoon periods with the latter generally deeper and more pronounced, as observed elsewhere (e.g., Fennel and Boss, 2003; see also review by Cullen, 2015). Interestingly, when POC and chlorophyll concentrations are vertically integrated the values can be higher during the spring intermonsoon than during the SWM because of the strong subsurface POC and chlorophyll maxima that develop during the spring intermonsoon (Gunderson, et al., 1998).

In the Arabian Sea, POC export normalized to 2000 meters ranges from < 6 to > 22 mgC m^{-2} d^{-1} (equal to < 0.5 to > 1.8 mmolC m^{-2} d^{-1}) depending upon location and season (Rixen et al., 2019; Honjo et al., 1999). In contrast, POC export from the base of the euphotic zone in the western Arabian Sea estimated from the satellite-derived net primary production data and export fluxes calculated with a model give 258.3 and 335.7 mgC m^{-2} d^{-1} (equal to 21.5 and 27.9 mmolC m^{-2} d^{-1}), respectively (Sreeush et al., 2018), suggesting dramatic declines in export at depth compared to the surface. The POC fluxes are generally highest in the western Arabian Sea during the SWM (>20 mgC m^{-2} d^{-1} equal to > 1.7 mmolC m^{-2} d^{-1}) where large seasonal variations in flux (7-24 mgC m^{-2} d^{-1} = 0.6-2 mmolC m^{-2} d^{-1}) are also observed (Honjo et al., 1999; Rixen et al., 2019b). In contrast, POC fluxes at 2000 meters are generally much lower in the central Arabian Sea (4-12 mgC m^{-2} d^{-1} = 0.25-0.5 mmolC m^{-2} d^{-1}) with the highest fluxes (> 10 mgC m^{-2} d^{-1} equal to > 0.8 mmolC m^{-2} d^{-1}) also occurring during SWM, though with much less pronounced seasonal variations (Rixen et al., 2019; Honjo et al., 1999). These patterns of POC flux in the Arabian Sea are broadly consistent with organic carbon burial and sediment accumulation rates calculated by Janke (1996), though with the latter an order of magnitude lower (Figure 9; <5 to >50 mmolC m^{-2} yr^{-1} which is equal to <0.01 to > .14 mmolC m^{-2} d^{-1}). Major flux events are also observed in the western Arabian Sea during both the SWM and NEM in association with passing eddies and wind-curl events; these events can dominate the annual mass flux (Honjo et al., 1999). ^{234}Th-estimated POC export fluxes in the Arabian Sea reveal similar spatial and temporal patterns with POC export efficiencies varying from <2 to 5% (Subha Anand et al, 2018a,b).

3.4.2 Bay of Bengal

Some of the highest concentrations of DOC in the Bay of Bengal (75-100 µmolC/kg) are observed in the near-surface (< 50 meters) waters of the northern Bay of Bengal, primarily due to the large inputs of fresh water and terrigenous DOC from rivers (Hansell, 2009; Shah et al., 2018; Figure 7). In addition, this fresh water enhances near-surface stratification which helps to maintain the elevated DOC concentrations because it inhibits vertical mixing, as discussed above. The concentration of DOC in the upper ocean in the Bay of Bengal also exhibits a significant relationship with Chlorophyll-a, POC and DOC exudation rates, suggesting possible sources through in situ biological processes (Rao and Sarma, 2022). Elevated DOC concentrations are also observed to > 200 meters depth in the Bay of Bengal due to the remineralization of sinking POM from the surface waters (Shah et al., 2018; Figure 7). Near-surface DOC concentrations tend to decline at lower latitudes (<14°N, Hansell, 2009; Shah et al., 2018). Rao et al. (2021) report that about half of the primary production in the Bay of Bengal is released as DOC during the summer monsoon due to existence of oligotrophic conditions, warm waters and dominance of picophytankton biomass and Shah et al. (2018) estimate that DOC remineralization fuels ~18% of the apparent oxygen utilization. As observed in the Arabian Sea, DOC concentrations below 500 meters in the Bay of Bengal are low (<50 µmolC/kg) and relatively uniform across the basin, and there appears to be little impact of the OMZ on DOC concentrations (Figure 7).

In the Bay of Bengal, the near-surface concentrations of POC can vary from < 4 to > 10 µmol/kg depending on location and season (Fernandes et al., 2009; Figure 12). Spatial and temporal variations are smaller compared to the Arabian Sea with POC concentrations varying from 4.3 to 11.1 µmolC/kg, 3.1 to 10.9 µmolC/kg, and 4.3 to 9.0 µmolC/kg during SWM, fall intermonsoon, and spring intermonsoon, respectively, in one study (Fernandes et al. 2009). In contrast to the Arabian Sea, POC and chlorophyll concentrations can be higher offshore compared to coastal stations in the Bay of Bengal, especially during SWM (Fernandes et al., 2009; Vinayachandran, 2009; Thushara et al., 2019). These elevated offshore POC and chlorophyll concentrations are not, however, revealed by remote sensing. Rather, the satellite estimates generally indicate that the highest concentrations occur near the coast (Gardner et al., 2006; Figure 8). As in the Arabian Sea, POC and chlorophyll concentrations are correlated in the Bay of Bengal with subsurface chlorophyll maxima generally deeper and more pronounced, as discussed above (e.g., Fernandes et al., 2009). In general, POC concentrations and percent POC contribution to the total suspended particulate matter tends to decrease with increasing water column depth indicating heterotrophic remineralization of sinking particles (Fernandes et al., 2009). High chlorophyll concentrations and high Chl*a*/POC ratios observed during the SWM and fall intermonsoon indicate the presence of relatively fresh POM in the Bay Bengal during these two seasons (Fernandes et al., 2009). POC concentration measured during the spring intermonsoon were lowest in the southern Bay of Bengal (0.51–0.65 µmolC/kg, Subha Anand et al., 2017). In general, seasonal and spatial differences in river influence, combined with physical forces such as eddies and mixing/entrainment that pump nutrients into the euphotic zone, drive seasonal and spatial variations in the quantity and quality of POM in the Bay of Bengal (Fernandes et al., 2009; Vinayachandran, 2009; Subha Anand et al., 2017; Thushara et al., 2019).

POC export normalized to 2000 meters in the Bay of Bengal is generally lower and less strongly seasonal than in the Arabian Sea, with fluxes varying between 2 and 14 mgC m^{-2} d^{-1} (= 0.17 – 1.2 mmolC m^{-2} d^{-1}; Rixen et al., 2019b). In contrast, POC export from the euphotic zone in the Sri Lanka Dome region estimated from the satellite-derived net primary production data and export fluxes calculated with a model give 118.5 and 427.4 mgC m^{-2} d^{-1} (equal to 9.8 and 35.6 mmolC m^{-2} d^{-1}), respectively (Sreeush et al., 2018), again suggesting dramatic declines in export at depth compared to the surface. In general, riverine freshwater and nutrient inputs to the Bay of Bengal increase POC export near the coast. This pattern is revealed by ^{234}Th-estimated POC export flux in the Bay of Bengal during the NEM, which varies from 0.1 to 1.6 mmolC m^{-2} d^{-1} with the highest flux observed in the east Indian coastal zone (Subha Anand et al., 2017). These patterns of POC flux are also broadly consistent with organic carbon burial and sediment accumulation rates calculated by Janke (1996), where the former are highest along the east coast of India (Figure 9). Though, as in the Arabian Sea, the organic carbon burial rates estimated by Janke (1996) are an order of magnitude lower than the POC fluxes normalized to 2000 meters from Rixen et al. (2019).

3.4.3 Equatorial waters, Indonesian Throughflow, and the Leeuwin Current

A modeling study reported by Hansell (2009) and Hansell et al. (2009) suggests a zonal decline in near-surface (30 meter) DOC concentrations along the equator in the Indian Ocean with values dropping from ~75 µmolC/kg in the east off of northern Sumatra to < 70 µmolC/kg in the west off of central east Africa. This pattern appears to be linked to the aforementioned declines in near-surface DOC concentrations to < 70 µmolC/kg that are associated with upwelling along the western side of the basin (Hansell and Peltzer, 1998; Hansell, 2009). The modeling study reported by Hansell (2009) and Hansell et al. (2009) also suggests that near-surface DOC concentrations are elevated to > 75 µmolC/kg in an open ocean region between 10° and 20°S and 80° and 100°E coincident with shallow OMZ (Figure 1), minimum sedimentation rate (Figure 9), and lower salinity (Figure 5), and that concentrations decline eastward to < 70 µmolC/kg in the the Indonesian Throughflow region and in the Leeuwin Current, but these features are not readily apparent in meridional or zonal sections (Figure 7). DOC concentrations below 500 meters in these waters are also low (<50 µmolC/kg) and uniform (Figure 7).

Satellite-estimated near-surface POC concentrations in open ocean equatorial waters of the Indian Ocean are generally low (< 60 mgC m^{-3} which is equal to < 5 µmolC/kg) with concentrations increasing during the SWM, especially in the west due to the aforementioned influence of coastal upwelling (Gardner et al., 2006; Figure 8). Elevated POC concentrations (> 72 mgC/m^3 which is equal to > 6 µmolC/kg) are also observed in the eastern equatorial Indian Ocean along the coast off Sumatra and Java and in the Indonesian Throughflow region, particularly during the SEM. All of these regions of elevated POC are associated with elevated chlorophyll concentrations (> 0.4% of POC; Figure 8, Gardner et al., 2006). Unsurprisingly, POC and chlorophyll concentrations are generally low along the coast of western Australia where the downwelling Leeuwin Current flows southward (Figure 8). Estimated organic carbon burial rates show similar patterns, i.e., low rates (< 5 mmolC m^{-2} yr^{-1}) in open ocean equatorial waters and higher rates in the west and east in association with upwelling and the influence of the Indonesian Throughflow (Janke, 1996; Figure 9). Surprisingly, estimated organic carbon burial rates are distinctly elevated (5-10 mmolC m^{-2} yr^{-1}) along the coast of Western Australia (Janke, 1996; Figure 9), likely due to coastal mixing processes, intermittent localized upwelling and eddy generation in the otherwise oligotrophic downwelling Leeuwin Current (Hood et al., 2017).

^{234}Th-estimates of POC export flux have revealed elevated values in eastern-central equatorial waters of the Indian Ocean during spring intermonsoon (up to 7.7 mmolC m^{-2} d^{-1}) in association with elevated rates of primary production (Subha Anand et al., 2017). These elevated rates are somewhat surprising given the downwelling circulation that is associated with the eastward-flowing equatorial currents (Strutton et al., 2015), but they are consistent with eastward increases in organic carbon burial and sedimentation rates along the equator (Janke, 1996; Figure 9). They are also consistent with eastward increases POC export from the euphotic zone estimated from the satellite-derived net primary production data and export fluxes calculated with a model that give 149.4 and 590.5 mgC m^{-2} d^{-1} (equal to 12.54 and 49.2 mmolC m^{-2} d^{-1}), respectively, off Sumatra, compared to similarly estimated values of 110.8 and 220.1 mgC $m^{-2}d^{-1}$ (equal to 9.2 and 18.3 mmolC m^{-2} d^{-1}), respectively, in the Seychelles-Chagos Thermocline Ridge region (Sreeush et al., 2018).

There are few direct measurements of POC concentrations and export flux off of western Australia. Waite et al. (2016) has shown that mesoscale eddies generated by the Leeuwin Current can strongly impact carbon export fluxes. Specifically, the subsurface distribution of particles in these eddies funnel into a wineglass shape down to 1000 m (Figure 13), leading to a sevenfold increase of vertical carbon flux in the eddy center versus the eddy flanks. This is consistent with the aforementioned idea that eddy generation in the Leeuwin Current gives rise to elevated organic carbon burial rates along the coast of Western Australia (Janke, 1996; Figure 9).

3.4.4 Southwestern Indian Ocean

Although the modeling study reported by Hansell (2009) and Hansell et al. (2009) suggests that near-surface (30 meter) DOC concentrations are lower (< 65 µmolC/kg) in the southwestern Indian Ocean and in the Mozambique Channel, these declines are not apparent in zonal sections (e.g., Figure 7). Rather, a meridional section along ~30° E (IO6N from Arctica to western South Africa) shows a very clear increase in near-surface (< 50 meter) DOC concentrations north of 45° S from < 50 µmolC/kg to >70 µmolC/kg (Hansel, 2009; Figure 7). Moreover, these elevated concentrations extend downward to > 300 meters depth (Figure 7). These data suggest that the Agulhas Current advects relatively high tropical and subtropical DOC concentrations southwestward along the coast of South Africa and also eastward in the Agulhas Retroflection, and that these elevated concentrations are being mixed downward in the current. This speculation is consistent with the fact that the Agulhas Current extends to >1000 meters depth and is derived from oligotrophic tropical and subtropical sources waters (Hood et al., 2017) that have relatively high DOC concentrations (Figure 7). DOC concentrations below 1000 meters in these waters are low (<50 μmolC/kg) and relatively uniform (Figure 7).

Satellite estimates suggest that POC concentrations are generally low (< 72 mgC m^{-3} which is equal to < 6 μmolC/kg) in the southwestern Indian Ocean and in the Agulhas Current during both the austral summer and winter seasons (Gardner et al., 2006; Figure 8). But some elevated POC concentrations (> 72 mgC/m^3, > 6 μmolC/kg) are observed in the austral winter in the Mozambique Channel, along the southwestern coast of South Africa, over the Agulhas Bank and in the Agulhas retroflection (Gardner et al., 2006; Figure 8). All of these regions are associated with elevated chlorophyll concentrations (> .4% of POC; Figure 8, Gardner et al., 2006). In the Mozambique Channel the elevated concentrations are associated with entrainment and offshore advection of coastal POM in eddies (Kolasinsky et al., 2012), whereas the elevated POM concentrations along the southwestern coast of South Africa and over the Agulhas Bank are associated with wind-induced and topographically controlled coastal upwelling (Hood et al., 2017; Hood et al., 2021, this volume). The tongue of elevated POC and chlorophyll concentration that is associated with the Agulhas retroflection is particularly striking (Figure 8). This is a region where strong eastward flows and persistent eddies are observed (Pazan and Niiler, 2004). It is possible that these eddies mix or upwell nutrients into the euphotic zone, fueling a low level of primary production. This region of elevated POC and chlorophyll extends all the way to the Kerguelen Islands during the austral summer (Figure 8; Gardner et al., 2006).

Estimated organic carbon burial rates in the southwestern Indian Ocean range from < 5 - ~10 mmolC m^{-2} yr^{-1} with the highest rates observed along the coastal zone of southeastern Africa (Janke, 1996; Figure 9). Interestingly, these estimates also clearly show elevated organic carbon burial (and sedimentation) rates in the same region where there is a tongue of elevated near-surface POC and chlorophyll concentration associated with the Agulhas retroflection (Gardner et al., 2006; compare Figures 8 and 9). These elevated carbon burial rates also extend all the way to the Kerguelen Islands. This is in contrast to the low carbon burial rates (< 5 mmolC m^{-2} yr^{-1}; Janke, 1996; Figure 9) and low ^{234}Th-estimated POC export fluxes (from 0.10 to 2.53 mmolC m^{-2} d^{-1} below 100m) that are observed slightly further south (Coppola et al., 2005).

3.4.5 Southern subtropical gyre

Near surface (< 50 meters) DOC concentrations in the southern subtropical gyre of the Indian Ocean are significantly elevated (> 75 μmolC/kg) between 10° and 35° S (Figure 7), consistent with the positive correlation between DOC concentrations and temperature, i.e., the southern subtropical gyre is warm and stratified and DOC concentrations become elevated because there is reduced vertical mixing. Near-surface DOC concentrations decline precipitously to < 50 μmolC/kg south of 40° S due to increased vertical mixing in the higher latitude waters (Figure 7). There is also evidence of subduction and northward transport of DOC in the subtropical front between 10° and 35° S where elevated DOC concentrations can be seen extending to > 250 meters depth (Figure 7). The source of this subducted water has DOC concentrations between 65 and 70 μmolC/kg, and as this water moves downward and equatorward the DOC is remineralized, dropping to ~55 μmolC/kg at 250 meters depth (Hansell, 2009; Figure 7). DOC concentrations below 500 meters in the southern subtropical Indian Ocean are also low (<50 μmolC/kg) and relatively uniform (Figure 7).

The lowest POC concentrations (< 48 mgC/m^3 equal to < 4 umolC/kg) in the Indian Ocean are observed in the oligotrophic southern subtropical gyre. These low POC values are associated with low chlorophyll concentrations (< .3% of POC; Figure 8, Gardner et al., 2006). These low POC and low percent chlorophyll waters dramatically increase in area during the Southern Hemisphere summer due to increases in summer stratification and lower nutrient availability (Gardner et al., 2006; Figure 8). Nonetheless, subsurface chlorophyll maxima exist below these oligotrophic regions (see Hood et al., 2022, this volume). It is likely that the subsurface chlorophyll maxima are associated with somewhat shallower subsurface POC maxima, with the latter weaker as discussed above.

Sediment trap-measured POC fluxes in the southern subtropical gyre of the Indian Ocean are some of the lowest recorded worldwide (~0.50 mgC m^{-2} day^{-1} = 0.04 mmolC m^{-2} d^{-1}, measured at 500–600 and 2600–3500 meters; Harms et al., 2021). Low POC fluxes are consistent with the extremely low organic carbon burial (< 2 mmolC m^{-2} yr^{-1}) and sediment accumulation rates calculated by Janke (1996; Figure 9). These low POC fluxes are the result of the strongly stratified, nutrient-depleted and low productivity near-surface waters in the gyre (Harms et al., 2021; Hood et al., 2022; this volume). These continuously oligotrophic conditions result in an almost constant POC fluxes in space and time. The lack of seasonality in the POC fluxes can also be attributed to intense organic matter degradation in the water column (Harms et al., 2021). The small amount of variability that is observed is related to variations wind-induced physical mixing events and the passage of eddies. Preliminary estimates indicate that the average POC export efficiency is extremely low (~0.03%) in these waters (Harms et al., 2021).

5. Summary and conclusions

The thickest OMZ in the world is found in the northern Indian Ocean in the Arabian Sea where intermediate water (~200-800 m) oxygen concentrations decline to nearly zero, with consequent impacts on nitrogen cycling. These impacts include denitrification-driven reductions in deep NO_3^- concentrations, appearance of NO_2^- maxima, generation of greenhouse gases (N_2O) and globally-significant losses of fixed nitrogen from the ocean. In contrast, these biogeochemical impacts are not observed in the Bay of Bengal where intermediate water dissolved oxygen concentrations are poised just above the threshold below which denitrification becomes significant. The low oxygen conditions in the water column in both the Arabian Sea and the Bay of Bengal are associated with slow ventilation and high biological oxygen demand. It appears that a weaker ballast effect and higher biological productivity sustain higher biological oxygen consumption in the Arabian Sea compared to the Bay of Bengal, which balances the higher physical oxygen supply in the Arabian Sea and explains its more intense OMZ.

The volume of hypoxic waters and denitrification in the Arabian Sea strongly increase in response to increases in monsoon winds. Such increases in Arabian Sea denitrification are expected to cause increases in N_2 and N_2O production. However, global syntheses of long term OMZ variability reveal only a weak decrease of dissolved oxygen concentrations in the OMZs of the Arabian Sea and the Bay of Bengal in comparison to OMZs of the South Atlantic Ocean and the Pacific Ocean. Moreover, outbreaks of hydrogen sulfide have so far not been reported in the northern Indian Ocean during the last 50 years, other than in bottom waters on the Indian shelf.

The absence of H_2S implies that the interplay between physical oxygen supply and the biological oxygen consumption has largely maintained the current hypoxic/anoxic conditions in the Arabian Sea and the Bay of Bengal OMZs. However, recent observational and modeling studies indicate that oxygen concentrations are now decreasing in the Arabian Sea and that these decreases are having significant biogeochemical and ecological impacts. Future evolution of the northern Indian Ocean OMZs projected by Earth System models is highly uncertain.

The Indian Ocean remains one of the most poorly sampled ocean regions with respect to inorganic and organic carbon pools and air-sea carbon fluxes. The system accounts for ~20% of the global oceanic uptake of atmospheric CO_2. The Arabian Sea is a source of CO_2 to the atmosphere due to elevated pCO_2 within the SWM-driven upwelling whereas it is still uncertain whether the Bay of Bengal is a CO_2 source or sink due to the sparse spatial and temporal sampling. South of 14°S the Indian Ocean appears to be a strong net CO_2 sink due to the combined effects of both the solubility pump and the biological pump. Surface pH values in the Indian Ocean are among the lowest of the major ocean basins, and the reasons for this are poorly understood. Increases in sulphate and nitrogen aerosol loadings over the Bay of Bengal may be mainly responsible for the increased acidity in the northwestern Bay of Bengal in recent years and reduced river discharge together with a positive IOD event have also been shown to contribute to enhanced acidification and pCO_2 levels in the coastal waters in the western Bay of Bengal. Projected increases in oceanic CO_2 concentrations will lead to further acidification of the Indian Ocean over the coming decades, with potentially severe negative impacts on coral reefs and other calcifying organisms.

DOC concentrations in the Indian Ocean vary between ~40 and 80 µmolC/kg. DOC concentrations in the Indian Ocean tend to be high in stratified near-surface tropical and subtropical waters where DOC is produced and accumulates, and DOC concentrations are lowest in the deep ocean where heterotrophic consumption of DOC exceeds autotrophic production. As observed elsewhere in the global ocean, satellite-estimated near-surface POC concentrations are elevated in coastal regions of the Indian Ocean with values often exceeding 120 mgC/m^3 (= 10 µmolC/kg). The highest POC concentrations in the Indian Ocean are observed in the northwestern part of the basin in the Arabian Sea and off the coast of Somalia with values estimated to be greater than 96 mgC/m^3 (= 8 µmolC/kg). These high POC values are associated with high chlorophyll concentrations. The lowest POC concentrations (< 48 mgC/m^3 = 4 µmolC/kg) are observed in the oligotrophic southern subtropical gyre. These low POC values are associated with low chlorophyll concentrations.

The spatial and temporal variability in POC export flux in the Indian Ocean is similar to the above mentioned patterns in POC and chlorophyll concentration, consistent with primary production as the main control on the spatial and temporal variability of organic carbon fluxes. However, in river-influence regions, like the Bay of Bengal, the spatial variability of organic carbon flux is also strongly influenced by lithogenic matter content. In the Arabian Sea POC export at 2000 meters ranges from < 6 to > 22 mgC m^{-2} d^{-1} (< 0.5 to > 1.8 mmolC m^{-2} d^{-1}) with the highest fluxes observed during the SWM. In contrast, POC export at 2000 meters in the Bay of Bengal is generally lower and less strongly seasonal than in the Arabian Sea with fluxes varying between 2 and 14 mgC m^{-2} d^{-1} (0.17 to 1.1 mmolC m^{-2} d^{-1}). ^{234}Th-estimates of POC export flux have revealed elevated values in eastern-central equatorial waters of the Indian

Ocean (up to 7.7 mmolC m^{-2} d^{-1}) in association with elevated rates of primary production. These elevated rates are surprising given the downwelling equatorial circulation, but they are consistent with zonal variations in satellite and model-based estimates of near surface POC export flux and organic carbon burial rates. There are few direct measurements of POC concentrations and export flux off of Western Australia where estimated organic carbon burial rates are distinctly elevated, perhaps due to the influence of Leeuwin Current eddies. Estimated organic carbon burial rates in the southwestern Indian Ocean range from < 5 - ~10 mmolC m^{-2} yr^{-1}, with the highest rates observed along the coastal zone of southeastern Africa and in the Agulhas retroflection. POC export fluxes in the southern subtropical gyre of the Indian Ocean are some of the lowest recorded worldwide (~0.50 mgC m^{-2} d^{-1} = 0.04 mmolC m^{-2} d^{-1}).

As in the other ocean basins, it is clear that there is a strong connection in the Indian Ocean between the physics that drives (or suppresses) nutrient delivery to the photic zone and responses of oxygen, CO_2 flux, pH, DOC, POC and POC export. Monsoonal wind forcing is a major driver of biogeochemical variability throughout the northern Indian Ocean and in equatorial waters. In addition, there are regionally specific processes that significantly modulate oxygen, CO_2 flux, pH, DOC, POC and POC export. For example, upwelling and strong advective impacts in the Arabian Sea; freshwater and stratification in the Bay of Bengal; the influence of ITF, poleward transport, downwelling and eddies in the southeastern Indian Ocean; and poleward transport of tropical waters, combined with localized upwelling in the southwestern Indian Ocean. The southern subtropical gyre is extremely oligotrophic.

Observational and modeling research should be aimed at improving understanding of northern Indian Ocean OMZ variability at seasonal and decadal time scales. Further, uncertainty in future projections needs to be reduced. Additional observations are also needed to better constrain air-sea CO_2 fluxes and the carbon cycle in general. Measurements of CO_2 and DOC concentrations, capturing spatial and temporal variability, are particularly sparse. This improved understanding is needed to predict the impacts of anthropogenic influence and global warming on Indian Ocean biogeochemistry and ecosystems and also for understanding the role of the Indian Ocean in global ocean biogeochemical cycles both now and in the future.

6. Educational Resources

-Ocean Data View, free software for plotting oceanographic data. Available at: https://odv.awi.de

-World Ocean Atlas, a collection of objectively analyzed, quality controlled temperature, salinity, oxygen, phosphate, silicate, and nitrate means based on profile data from the World Ocean Database. Available at: https://www.ncei.noaa.gov/products/world-ocean-atlas

-Surface Ocean CO_2 Atlas (SOCAT) is a synthesis of quality-controlled, surface ocean fCO_2 (fugacity of carbon dioxide) observations by the international marine carbon research community. Available at: https://www.socat.info

-Satellite ocean color data. Available at: https://oceancolor.gsfc.nasa.gov

Acknowledgements

The development of this article was supported by the Scientific Committee for Oceanic Research (SCOR) via direct funding to the Second International Indian Ocean Expedition (IIOE-2) and indirect funding through the Integrated Marine Biosphere Research (IMBeR) regional program SIBER (Sustained Indian Ocean Biogeochemistry and Ecosystem Research). Additional support was provided by NASA grant no. 80NSSC17K0258 49A37A, NOAA grant no. NA15NMF4570252 NCRS-17, and NSF grant no. 2009248 to R. Hood. The Ocean Data View software package (https://odv.awi.de) was used in developing this article's original graphics. The article also benefitted from extensive comments provided by Dr. V.V.S.S. Sarma and one anonymous reviewer. This is UMCES contribution YYYY.

Author contributions

All authors contributed to writing of the text, discussion of content, and structure of the chapter.

Index Terms

Indian Ocean, Arabian Sea, Bay of Bengal, Indonesian Throughflow, Leeuwin Current, Mozambique Channel, Agulhas Current, Indian Ocean southern subtropical gyre, oxygen, oxygen minimum zone, salinity, stratification, denitrification, N_2O, CO_2, pH, dissolved organic carbon (DOC), particulate organic carbon (POC), carbon export flux.

References

Acharya, Shiba Shankar, and Mruganka K Panigrahi. 2016. 'Eastward shift and maintenance of Arabian Sea oxygen minimum zone: Understanding the paradox', *Deep Sea Research Part I: Oceanographic Research Papers*, 115: 240-52.

Al Azhar, Muchamad, Zouhair Lachkar, Marina Lévy, and Shafer Smith. 2017. 'Oxygen minimum zone contrasts between the Arabian Sea and the Bay of Bengal implied by differences in remineralization depth', *Geophysical Research Letters*, 44: 11,106-11,14.

Altabet, M. A., R. Francois, D. W. Murray, and W. L. Prell. 1995. 'Climate-related variations in denitrification in the Arabian Sea from sediment N-15/N-14 ratios', *Nature*, 373: 506-09.

Altabet, Mark A, Matthew J Higginson, and David W Murray. 2002. 'The effect of millennial-scale changes in Arabian Sea denitrification on atmospheric CO 2', *Nature*, 415: 159-62.

Altieri, Andrew H, Seamus B Harrison, Janina Seemann, Rachel Collin, Robert J Diaz, and Nancy Knowlton. 2017. 'Tropical dead zones and mass mortalities on coral reefs', *Proceedings of the National Academy of Sciences*, 114: 3660-65.

Anand, S Subha, R Rengarajan, Damodar Shenoy, Mangesh Gauns, and SWA Naqvi. 2018. 'POC export fluxes in the Arabian Sea and the Bay of Bengal: A simultaneous 234Th/238U and 210Po/210Pb study', *Marine Chemistry*, 198: 70-87.

Anju, M, V Valsala, BR Smitha, G Bharathi, and CV Naidu. 2022. 'Observed denitrification in the northeast Arabian Sea during the winter-spring transition of 2009', *Journal of Marine Systems*, 227: 103680.

Antoine, David, Jean-Michel André, and André Morel. 1996. 'Oceanic primary production: 2. Estimation at global scale from satellite (coastal zone color scanner) chlorophyll', *Global Biogeochemical Cycles*, 10: 57-69.

Bahl, A, A Gnanadesikan, and M-A Pradal. 2019. 'Variations in ocean deoxygenation across earth system models: Isolating the role of parameterized lateral mixing', *Global Biogeochemical Cycles*, 33: 703-24.

Bakker, D. C. E., and et al. 2014. 'An update to the Surface Ocean CO2 Atlas (SOCAT version 2)', *Earth Systems Science Data*, 6: 69-90.

Bange, H. W., and et. al. 2000. 'A revised nitrogen budget for the Arabian Sea', *Global Biogeochemical Cycles*, 14: 1283-97.

Bange, Hermann W, MO Andreae, S Lal, CS Law, SWA Naqvi, PK Patra, T Rixen, and RC Upstill-Goddard. 2001. 'Nitrous oxide emissions from the Arabian Sea: A synthesis', *Atmospheric Chemistry and Physics*, 1: 61-71.

Banse, K, SWA Naqvi, PV Narvekar, JR Postel, and DA Jayakumar. 2014. 'Oxygen minimum zone of the open Arabian Sea: variability of oxygen and nitrite from daily to decadal timescales', *Biogeosciences*, 11: 2237-61.

Bates, N. R., A. C. Pequignet, and C. L. Sabine. 2006. 'Ocean carbon cycling in the Indian Ocean: I. Spatio-temporal variability of inorganic carbon and air-sea CO_2 gas exchange', *Global Biogeochemical Cycles*, 20: GB3020.

Bednarsek, N., G. A. Tarling, D. C. E. Bakker, S. Fielding, E. M. Jones, H. J. Venables, P. Ward, A. Kuzirian, B. Leze, R. A. Feely, and E. J. Murphy. 2012. 'Extensive dissolution of live pteropods in the Southern Ocean', *Nature Geoscience*, 5: 881-85.

Behrman, D. 1981. *Assault on the Largest Unknown: the International Indian Ocean Expedition, 1959-1965* (UNESCO Press: Paris).

Bercovici, SK, AP McNichol, L Xu, and DA Hansell. 2018. 'Radiocarbon content of dissolved organic carbon in the South Indian Ocean', *Geophysical Research Letters*, 45: 872-79.

Bopp, L, Laure Resplandy, A Untersee, P Le Mezo, and M Kageyama. 2017. 'Ocean (de)oxygenation from the Last Glacial Maximum to the twenty-first century: insights from Earth System models', *Philosophical Transactions of the Royal Society A: Mathematical, Physical and Engineering Sciences*, 375: 20160323.

Bopp, Laurent, Laure Resplandy, James C Orr, Scott C Doney, John P Dunne, M Gehlen, P Halloran, Christoph Heinze, Tatiana Ilyina, and Roland Seferian. 2013. 'Multiple stressors of ocean ecosystems in the 21st century: projections with CMIP5 models', *Biogeosciences*, 10: 6225-45.

Boyd, Philip W, Hervé Claustre, Marina Levy, David A Siegel, and Thomas Weber. 2019. 'Multi-faceted particle pumps drive carbon sequestration in the ocean', *Nature*, 568: 327-35.

Bristow, Laura A, Cameron M Callbeck, Morten Larsen, Mark A Altabet, Julien Dekaezemacker, Michael Forth, M Gauns, Ronnie N Glud, Marcel MM Kuypers, and Gaute Lavik. 2017. 'N_2 production rates limited by nitrite availability in the Bay of Bengal oxygen minimum zone', *Nature Geoscience*, 10: 24-29.

Cabré, Anna, Irina Marinov, Raffaele Bernardello, and Daniele Bianchi. 2015. 'Oxygen minimum zones in the tropical Pacific across CMIP5 models: mean state differences and climate change trends', *Biogeosciences*, 12: 5429-54.

Canfield, Don E, Beate Kraft, Carolin R Löscher, Richard A Boyle, Bo Thamdrup, and Frank J Stewart. 2019. 'The regulation of oxygen to low concentrations in marine oxygen-minimum zones', *Journal of Marine Research*, 77: 297-324.

Carruthers, JN, SS Gogate, JR Naidu, and T Laevastu. 1959. 'Shorewards upslope of the layer of minimum oxygen off Bombay: Its influence on marine biology, especially fisheries', *Nature*, 183: 1084-87.

Cerutti, Julia, April J Burt, Philip Haupt, Nancy Bunbury, Peter J Mumby, and Gabriela Schaepman-Strub. 2020. 'Impacts of the 2014–2017 global bleaching event on a protected remote atoll in the Western Indian Ocean', *Coral Reefs*, 39: 15-26.

Chakraborty, Kunal, Vinu Valsala, Trishneeta Bhattacharya, and Jayashree Ghosh. 2021. 'Seasonal cycle of surface ocean pCO2 and pH in the northern Indian Ocean and their controlling factors', *Progress in Oceanography*, 198: 102683.

Chakraborty, Kunal, Vinu Valsala, GVM Gupta, and VVSS Sarma. 2018. 'Dominant biological control over upwelling on pCO2 in sea east of Sri Lanka', *Journal of Geophysical Research: Biogeosciences*, 123: 3250-61.

Codispoti, L., J. A. Brandes, J. Christensen, A. Devol, S. Naqvi, H. W. Paerl, and T. Yoshinari. 2001. 'The oceanic fixed nitrogen and nitrous oxide budgets: Moving targets as we enter the anthropocene?', *Scientia Marina (Barcelona)*, 65, suppl. 2: 85-105.

Coppola, L, M Roy-Barman, S Mulsow, P Povinec, and C Jeandel. 2005. 'Low particulate organic carbon export in the frontal zone of the Southern Ocean (Indian sector) revealed by 234Th', *Deep Sea Research Part I: Oceanographic Research Papers*, 52: 51-68.

Cullen, John J. 2015. 'Subsurface chlorophyll maximum layers: enduring enigma or mystery solved?', *Annual Review of Marine Science*, 7: 207-39.

Dalsgaard, T., D. E. Canfield, J. Petersen, B. Thamdrup, and J. Acuna-Gonzalez. 2003. 'N_2 production by the anammox reaction in the anoxic water column of Golfo Dulce, Costa Rica', *Nature*, 422: 606-08.

de la Rocha, Christina, and Uta Passow. 2014. "The biological pump." In.: Elsevier Science.

de Moel, H., G. M. Ganssen, F. J. C. Peeters, S. J. A. Jung, D. Kroon, G. J. A. Brummer, and R. E. Zeebe. 2009. 'Planktonic foraminiferal shell thinniing in the Arabian Sea due to anthropogenic ocean acidification?', *Biogeosciences*, 6: 1917-25.

de Verneil, Alain, Zouhair Lachkar, Shafer Smith, and Marina Lévy. 2021. 'Evaluating the Arabian Sea as a regional source of atmospheric CO 2: seasonal variability and drivers', *Biogeosciences Discussions*: 1-38.

Deutsch, C., J. L. Sarmeinto, D. M. Sigman, N. Gruber, and J. P. Dunne. 2007. 'Spatial coupling of nitrogen inputs and losses in the ocean', *Nature*, 445: 163-67.

DeVries, T, C Deutsch, PA Rafter, and F Primeau. 2013. 'Marine denitrification rates determined from a global 3-D inverse model', *Biogeosciences*, 10: 2481-96.

Diaz, RJ, R Rosenberg, and K Sturdivant. 2019. 'Hypoxia in estuaries and semi-enclosed seas', *Ocean deoxygenation: Everyone's problem, edited by: Laffoley, D. and Baxter, JM, IUCN, Gland, Switzerland*.

Diaz, Robert J., and Rutger Rosenberg. 2008. 'Spreading Dead Zones and Consequences for Marine Ecosystems', *Science*, 321: 926-29.

Dietrich, GÜNTER. 1936. 'Aufbau und Bewegung von Golfstrom und Agulhasstrom, eine vergleichende Betrachtung', *Naturwissenschaften*, 24: 225-30.

Doney, S. C. 2010. 'The growing human footprint on coastal and open-ocean biogeochemistry', *Science*, 328: 1512-16.

Dueser, WG, EH Ross, and ZJ Mlodzinska. 1978. 'Evidence for and rate of denitrification in the Arabian Sea', *Deep Sea Research*, 25: 431-45.

Duteil, Olaf, and Andreas Oschlies. 2011. 'Sensitivity of simulated extent and future evolution of marine suboxia to mixing intensity', *Geophysical Research Letters*, 38.

Eugster, Olivier, and Nicolas Gruber. 2012. 'A probabilistic estimate of global marine N-fixation and denitrification', *Global Biogeochemical Cycles*, 26.

Fasham, Michael JR. 2003. 'JGOFS: a retrospective view.' in, *Ocean Biogeochemistry* (Springer).

Feely, R. A., S. C. Doney, and S. R. Cooley. 2009. 'Ocean acidification: Present conditions and future changes in a high-CO_2 world', *Oceanography*, 22: 36-47.

Feely, Richard A, Rik Wanninkhof, Simone Alin, John L Bullister, Gregory C Johnson, Jeremy Mathis, Calvin W Mordy, Molly Baringer, and Jia-Zhong Zhang. 2005. 'Global Repeat Hydrographic/CO2/Tracer Surveys in Support of CLIVAR and Global Cycle Objectives: Carbon Inventories and Fluxes'.

Fennel, Katja, and Emmanuel Boss. 2003. 'Subsurface maxima of phytoplankton and chlorophyll: Steady-state solutions from a simple model', *Limnology and Oceanography*, 48: 1521-34.

Fernandes, Loreta, Narayan B Bhosle, SG Prabhu Matondkar, and Ravi Bhushan. 2009. 'Seasonal and spatial distribution of particulate organic matter in the Bay of Bengal', *Journal of Marine Systems*, 77: 137-47.

Fine, Rana A. 1993. 'Circulation of Antarctic intermediate water in the South Indian Ocean', *Deep Sea Research Part I: Oceanographic Research Papers*, 40: 2021-42.

Fuhrman, Jed A, and Douglas G Capone. 1991. 'Possible biogeochemical consequences of ocean fertilization', *Limnology and Oceanography*, 36: 1951-59.

Garcia, H. E., R. A. Locarnini, T. P. Boyer, J. I. Antonov, M. M. Zweng, O. K. Baranova, and D. R. Johnson. 2010. 'World Ocean Atlas 2009', *S. Levitus (Ed.), NOAA Atlas NESDIS 71, Vol. 4, Washington, D. C., U.S. Government Printing Office*.

Gardner, WD, AV Mishonov, and MJ Richardson. 2006. 'Global POC concentrations from in-situ and satellite data', *Deep Sea Research Part II: Topical Studies in Oceanography*, 53: 718-40.

Gattuso, J.-P., and L. Hansson. 2011. *Ocean Acidification* (Oxford University Press: Oxford, UK).

Gaye, Birgit, Anna Böll, Joachim Segschneider, Nicole Burdanowitz, Kay-Christian Emeis, Venkitasubramani Ramaswamy, Niko Lahajnar, Andreas Lückge, and Tim Rixen. 2018. 'Glacial–interglacial changes and Holocene variations in Arabian Sea denitrification', *Biogeosciences*, 15: 507-27.

Gaye, Birgit, Birgit Nagel, Kirstin Dähnke, Tim Rixen, and Kay-Christian Emeis. 2013. 'Evidence of parallel denitrification and nitrite oxidation in the ODZ of the Arabian Sea from paired stable isotopes of nitrate and nitrite', *Global Biogeochemical Cycles*, 27: 1059-71.

Gilson, Hugh Cary. 1933. 'The nitrogen cycle', *The John Murray Expedition*, 1934: 21-81.

Gnanadesikan, A, JP Dunne, and J John. 2012. 'Understanding why the volume of suboxic waters does not increase over centuries of global warming in an Earth System Model', *Biogeosciences*, 9: 1159-72.

Goes, Joaquim I, and Helga do R Gomes. 2016. 'An ecosystem in transition: the emergence of mixotrophy in the Arabian Sea.' in, *Aquatic Microbial Ecology and Biogeochemistry: A Dual Perspective* (Springer).

Goes, Joaquim I, Hongzhen Tian, Helga do Rosario Gomes, O Roger Anderson, Khalid Al-Hashmi, Sergio deRada, Hao Luo, Lubna Al-Kharusi, Adnan Al-Azri, and Douglas G Martinson. 2020. 'ecosystem state change in the Arabian Sea fuelled by the recent loss of snow over the Himalayan-tibetan plateau region', *Scientific Reports*, 10: 1-8.

Gomes, H. D., J. I. Goes, S. G. P. Motondkar, E. J. Buskey, S. Basu, S. Parab, and P. G. Thoppil. 2014. 'Massive outbreaks of Notiluca scintillans blooms in teh Arabian Sea due to spread of hypoxia', *Nature Communications*, 5: http://dx.doi.org/10.1038/ncomms5862.

Gould, John, Bernadette Sloyan, and Martin Visbeck. 2013. 'In situ ocean observations: A brief history, present status, and future directions.' in, *International Geophysics* (Elsevier).

Graham, N. A. J., S. K. Wilson, S. Jennings, N. V. C. Polunin, J. Robinson, J. P. Bijoux, and T. M. Daw. 2007. 'Lag effects in the impacts of mass coral bleaching on coral reef fish, fisheries, and ecosystems', *Conservation Biology*, 21: 1291-300.

Gruber, N., and J. L. Sarmiento. 1997. 'Global patterns of marine nitrogen fixation and denitrification', *Global Biogeochemical Cycles*, 11: 235-66.

Gruber, Nicolas. 2004. 'The dynamics of the marine nitrogen cycle and its influence on atmospheric CO 2 variations.' in, *The ocean carbon cycle and climate* (Springer).

Gruber, Nicolas, and James N Galloway. 2008. 'An Earth-system perspective of the global nitrogen cycle', *Nature*, 451: 293-96.

Gundersen, J. S., W. D. Gardner, M. J. Richardson, and I. D. Walsh. 1998. 'Effects of monsoons on the seasonal and spatial distributions of POC and chlorophyll in the Arabian Sea', *Deep Sea Research Part II*, 45: 2103-32.

Gupta, GVM, R Jyothibabu, Ch V Ramu, A Yudhistir Reddy, KK Balachandran, V Sudheesh, Sanjeev Kumar, NVHK Chari, Kausar F Bepari, and Prachi H Marathe. 2021. 'The world’s largest coastal deoxygenation zone is not anthropogenically driven', *Environmental Research Letters*, 16: 054009.

Gupta, GVM, V Sudheesh, KV Sudharma, N Saravanane, V Dhanya, KR Dhanya, G Lakshmi, M Sudhakar, and SWA Naqvi. 2016. 'Evolution to decay of upwelling and associated biogeochemistry over the southeastern Arabian Sea shelf', *Journal of Geophysical Research: Biogeosciences*, 121: 159-75.

Gupta, R Sen, and SWA Naqvi. 1984. 'Chemical oceanography of the Indian Ocean, north of the equator', *Deep Sea Research Part A. Oceanographic Research Papers*, 31: 671-706.

Haake, B, and V Ittekkot. 1990. 'Die Wind-getriebene „biologische Pumpe” und der Kohlenstoffentzug im Ozean', *Naturwissenschaften*, 77: 75-79.

Hansell, Dennis A. 2009. 'Dissolved organic carbon in the carbon cycle of the Indian Ocean', *Indian Ocean Biogeochemical Processes and Ecological Variability, Geophys. Monogr. Ser*, 185: 217-30.

Hansell, Dennis A, Craig A Carlson, Daniel J Repeta, and Reiner Schlitzer. 2009. 'Dissolved organic matter in the ocean: A controversy stimulates new insights', *Oceanography*, 22: 202-11.

Hansell, Dennis A, and Mónica V Orellana. 2021. 'Dissolved Organic Matter in the Global Ocean: A Primer', *Gels*, 7: 128.

Hansell, Dennis A, and Edward T Peltzer. 1998. 'Spatial and temporal variations of total organic carbon in the Arabian Sea', *Deep Sea Research Part II: Topical Studies in Oceanography*, 45: 2171-93.

Harms, Natalie C, Niko Lahajnar, Birgit Gaye, Tim Rixen, Ulrich Schwarz-Schampera, and Kay-Christian Emeis. 2021. 'Sediment trap-derived particulate matter fluxes in the oligotrophic subtropical gyre of the South Indian Ocean', *Deep Sea Research Part II: Topical Studies in Oceanography*: 104924.

Helly, J. J., and L. A. Levin. 2004. 'Global distribution of naturally occurring marine hypoxia on continental margins', *Deep Sea Research Part I* 51: 1159-68.

Hoegh-Guldberg, O., and et. al. 2014. 'Chapter 30: The Ocean.' in IPCC WGII AR5 (ed.), *Climate Change 2014: Impacts, Adaptation, and Vulnerability. Contribution of Working Group II to the Fifth Assessment Report of the Intergovernmental Panel on Climate Change* (Cambridge University Press: Cambridge, UK, and New York, NY, USA).

Hoegh-Guldberg, O., P. J. Mumby, A. J. Hooten, R. S. Steneck, P. Greenfield, E. Gomez, C. D. Harvell, P. F. Sale, A. J. Edwards, K. Caldeira, N. Knowlton, C. M. Eakin, R. Iglesias-Prieto, N. Muthiga, R. H. Bradbury, A. Dubi, and M. E. Hatziolos. 2007. 'Coral reefs under rapid climate change and oceand acidification', *Science*, 318: 1737-42.

Honjo, S., J. Dymond, W. Prell, and V. Ittekkot. 1999. 'Monsoon-controlled export fluxes to the interior of the Arabian Sea', *Deep-Sea Research (Part II, Topical Studies in Oceanography)*, 46: 1859-902.

Hood, R. R. , H. W. Bange, L. Beal, L. E. Beckley, P. Burkill, G. L. Cowie, N. D'Adamo, G. Ganssen, H. Hendon, J. Hermes, M. Honda, M. McPhaden, M. Roberts, S. Singh, E. Urban, and W. Yu. 2015. "Science Plan of the Second International Indian Ocean Expedition (IIOE-2): A Basin-Wide Research Program." In. Newark, Delaware, USA: Scientific Committee on Oceanic Research.

Hood, R. R., L. E. B. Beckley, and J. D. Wiggert. 2017. 'Biogeochemical and ecological impacts of boundary currents in the Indian Ocean', *Progress in Oceanography*, 156: 290-325.

Hood, R. R., V. J. Coles, J. Huggett, M. Landry, M. Levy, and J. W. Moffett. 2021. 'Nutrient, phytoplankton and zooplankton variability in the Indian Ocean', *In: The Indian Ocean and its role in the global climate system, C. C. Ummenhofer and R. R. Hood (eds.), Elsevier*.

Howell, E. A., S. C. Doney, R. A. Fine, and D. B. Olson. 1997. 'Geochemical estimates of denitrification in the Arabian Sea and the Bay of Bengal during WOCE', *Geophysical Research Letters*, 24: 2549-52.

Hutchins, D. A., F.-X. Fu, Y. Zhang, M. E. Warner, Y. Feng, K. Portune, P. W. Bernhardt, and M. R. Mulholland. 2007. 'CO_2 control of Trichodesmium N_2 fixation, photosynthesis, growth rates, and elemental ratios: Implications for past, present, and future ocean biogeography', *Limnology and Oceanography*, 52: 1293-304.

IPCC. 2007. 'Contribution of Working Groups I, II and III to the Fourth Assessment Report of the Intergovernmental Panel on Climate Change.' in Core_Writing_Team, R. K. Pachauri and A. Reisinger (eds.) (IPCC: Geneva, Switzerland).

———. 2019. 'IPCC Special Report on the Ocean and Cryosphere in a Changing Climate'.

Ito, Takamitsu, Shoshiro Minobe, Matthew C Long, and Curtis Deutsch. 2017. 'Upper ocean O2 trends: 1958–2015', *Geophysical Research Letters*, 44: 4214-23.

Ittekkot, V, RR Nair, S Honjo, Vo Ramaswamy, M Bartsch, S Manganini, and BN Desai. 1991. 'Enhanced particle fluxes in Bay of Bengal induced by injection of fresh water', *Nature*, 351: 385-87.

Ivanenkov, VN, and AG Rozanov. 1966. *Hydrogen sulphide contamination of the intermediate layers of the Arabian Sea and the Bay of Bengal* (National Institute of Oceanography).

Jahnke, Richard A. 1996. 'The global ocean flux of particulate organic carbon: Areal distribution and magnitude', *Global Biogeochemical Cycles*, 10: 71-88.

Kolasinski, Joanna, Sven Kaehler, and Sébastien Jaquemet. 2012. 'Distribution and sources of particulate organic matter in a mesoscale eddy dipole in the Mozambique Channel (south-western Indian Ocean): Insight from C and N stable isotopes', *Journal of Marine Systems*, 96: 122-31.

Kumar, M Dileep, SWA Naqvi, MD George, and DA Jayakumar. 1996. 'A sink for atmospheric carbon dioxide in the northeast Indian Ocean', *Journal of Geophysical Research: Oceans*, 101: 18121-25.

Kuypers, M. M. M., A. O. Sliekers, G. Lavik, M. Schmid, B. B. Joergensen, J. G. Kuenen, J. S. S. Damste, M. Strous, and M. S. M. Jetten. 2003. 'Anaerobic ammonium oxidation by anammox bacteria in the Black Sea', *Nature*, 422: 608-11.

Kwiatkowski, Lester, Olivier Torres, Laurent Bopp, Olivier Aumont, Matthew Chamberlain, James R Christian, John P Dunne, Marion Gehlen, Tatiana Ilyina, and Jasmin G John. 2020. 'Twenty-first century ocean warming, acidification, deoxygenation, and upper-ocean nutrient and primary production decline from CMIP6 model projections', *Biogeosciences*, 17: 3439-70.

Lachkar, Zouhair, Marina Lévy, and K Shafer Smith. 2019. 'Strong intensification of the Arabian Sea oxygen minimum zone in response to Arabian Gulf warming', *Geophysical Research Letters*, 46: 5420-29.

Lachkar, Zouhair, Marina Lévy, and Shafer Smith. 2018. 'Intensification and deepening of the Arabian Sea oxygen minimum zone in response to increase in Indian monsoon wind intensity', *Biogeosciences*, 15: 159-86.

Lachkar, Zouhair, Michael Mehari, Muchamad Al Azhar, Marina Lévy, and Shafer Smith. 2020. 'Fast local warming of sea-surface is the main factor of recent deoxygenation in the Arabian Sea', *Biogeosciences Discussions*: 1-27.

Lachkar, Zouhair, Shafer Smith, Marina Lévy, and Olivier Pauluis. 2016. 'Eddies reduce denitrification and compress habitats in the Arabian Sea', *Geophysical Research Letters*, 43: 9148-56.

Lévy, Marina, Laure Resplandy, Jaime B Palter, Damien Couespel, and Zouhair Lachkar. 2021. "The crucial contribution of mixing to present and future ocean oxygen distribution." In.: Elsevier.

Luyten, JR, Joseph Pedlosky, and Henry Stommel. 1983. 'The ventilated thermocline', *Journal of Physical Oceanography*, 13: 292-309.

McCartney, M. S. 1979. 'Subantarctic mode water', *Woods Hole Oceanographic Institution Contribution*, 3773: 103-19.

McClanahan, T. R., M. Ateweberhan, N. A. J. Graham, S. K. Wilson, C. R. Sebastian, M. M. M. Guillaume, and J. H. Bruggemann. 2007. 'Western Indian Ocean coral communities: bleaching responses and susceptibility to extinction', *Marine Ecology Progress Series*, 337: 1-13.

McCreary, J. P., Z. Yu, R. R. Hood, P. N. Vinayachandran, R. Furue, A. Ishida, and K. J. Richards. 2013. 'Dynamcis of the Indian-Ocean oxygen minumum zones', *Progress in Oceanography*, 112-113: 15-37.

McElroy, MB. 1983. 'Marine biological controls on atmospheric CO 2 and climate', *Nature*, 302: 328-29.

Moore, J. A., L. M. Bellchambers, M. R. Depczynski, R. D. Evans, S. N. Evans, S. N. Field, K. J. Friedman, J. P. Gilmour, T. H. Holmes, R. Middlebrook, B. T. Radford, T. Ridgway, G. Shedrawi, H. Taylor, D. P. Thompson, and S. K. Wilson. 2012. 'Unprecedented mass bleaching and loss of coral across 12 degrees of latitude in Western Australia in 2010-11', *PloS ONE*, 7: e51087, doi:10.1317/journal.pone.0051807.

Moore, Willard S. 1984. 'Review of the geosecs project', *Nuclear Instruments and Methods in Physics Research*, 223: 459-65.

Morrison, J. M., L. A. Codispoti, S. L. Smith, K. Wishner, C. Flagg, W. D. Gardner, S. Gaurin, S. W. A. Naqvi, V. Manghnani, L. Prosperie, and J. S. Gundersen. 1999. 'The oxygen minimum zone in the Arabian Sea during 1995', *Deep-Sea Research (Part II, Topical Studies in Oceanography)*, 46: 1903-31.

Naqvi, S Wajih A, Ronald J Noronha, and CV Gangadhara Reddy. 1982. 'Denitrification in the Arabian Sea', *Deep Sea Research Part A. Oceanographic Research Papers*, 29: 459-69.

Naqvi, S. W. A. 1991. 'Geographical extent of denitrification in the Arabian Sea in relation to some physical processes', *Oceanologica Acta*, 14: 281-90.

———. 2019. 'Evidence for ocean deoxygenation and its patterns: Indian Ocean', *Ocean deoxygenation: Everyone's problem, edited by: Laffoley, D. and Baxter, JM, IUCN, Gland, Switzerland*.

Naqvi, S. W. A., H. W. Bange, S. W. Gibb, C. Goyet, A. D. Hatton, and R. C. Upstill-Goddard. 2005. 'Biogeochemical ocean-atmosphere transfers in the Arabian Sea', *Progress in Oceanography*, 65: 116-44.

Naqvi, S. W. A., D. A. Jayakumar, P. V. Narvekar, H. Naik, Vvss Sarma, W. D'Souza, S. Joseph, and M. D. George. 2000. 'Increased marine production of N_2O due to intensifying anoxia on the Indian continental shelf', *Nature*, 408: 346-49.

Newell, BS. 1969. 'Seasonal variations in the Indian Ocean along 110° E. II. Particulate carbon', *Marine and Freshwater Research*, 20: 51-54.

Obura, David, Mishal Gudka, F Abdou Rabi, S Bacha Gian, L Bigot, J Bijoux, S Freed, J Maharavo, V Munbodhe, and J Mwaura. 2017. 'Coral reef status report for the Western Indian Ocean. Global Coral Reef Monitoring Network (GCRMN)', *International Coral Reef Initiative (ICRI)*, 144.

Paulmier, Aurélien, and Diana Ruiz-Pino. 2009. 'Oxygen minimum zones (OMZs) in the modern ocean', *Progress in Oceanography*, 80: 113-28.

Pazan, Stephen E, and Peter Niiler. 2004. "New global drifter data set available." In.: Wiley Online Library.

Piketh, S. J. , P. D. Tyson, and W. Steffen. 2000. 'Aeolian transport from southern Africa and iron fertilization of marine biota in the South Indian Ocean', *South African Journal of Science*, 96: 244-46.

Piontkovski, SA, and HS Al-Oufi. 2015. 'The Omani shelf hypoxia and the warming Arabian Sea', *International Journal of Environmental Studies*, 72: 256-64.

Queste, Bastien Y, Clément Vic, Karen J Heywood, and Sergey A Piontkovski. 2018. 'Physical controls on oxygen distribution and denitrification potential in the north west Arabian Sea', *Geophysical Research Letters*, 45: 4143-52.

Ramaswamy, V, RR Nair, Sl Manganini, B Haake, and V Ittekkot. 1991. 'Lithogenic fluxes to the deep Arabian Sea measured by sediment traps', *Deep Sea Research Part A. Oceanographic Research Papers*, 38: 169-84.

Ramaswamy, V., O. Boucher, J. Haigh, D. Hauglustaine, J. Haywood, G. Myhre, T. Nakajima, G. Y. Shi, and S. Solomon. 2001. 'Radiative Forcing of Climate Change.' in J. T. Houghton, Y. Ding, Griggs, D. J., M. Noguer, P. J. Van der Linden, X. Dai, K. Maskell and C. A. Johnson (eds.), *Climate Change 2001: The Scientific Basis: Contribution of Working Group I to the Third Assessment Report of the Intergovernmental Panel on Climate Change* (Cambridge University Press: Cambridge, U. K.).

Rao, CK, SWA Naqvi, M Dileep Kumar, SJD Varaprasad, DA Jayakumar, MD George, and SYS Singbal. 1994. 'Hydrochemistry of the Bay of Bengal: possible reasons for a different water-column cycling of carbon and nitrogen from the Arabian Sea', *Marine Chemistry*, 47: 279-90.

Rao, DN, M Chopra, GR Rajula, DSL Durgadevi, and VVSS Sarma. 2021. 'Release of significant fraction of primary production as dissolved organic carbon in the Bay of Bengal', *Deep Sea Research Part I: Oceanographic Research Papers*, 168: 103445.

Rao, DN, and VVSS Sarma. 2022. 'Accumulation of dissolved organic carbon and nitrogen in the photic zone in the nitrogen-depleted waters of the Bay of Bengal', *Marine Chemistry*, 239: 104074.

Rashid, T., S. Hoque, and F. Akter. 2013. 'Ocean acidification in the Bay of Bengal', *Scientific Reports*, 2: 699.

Resplandy, Laure. 2018. 'Climate change and oxygen in the ocean', *Nature: International Weekly Journal of Science*.

Resplandy, Laure, Marina Lévy, Laurent Bopp, Vincent Echevin, Stéphane Pous, VVSS Sarma, and D Kumar. 2012. 'Controlling factors of the oxygen balance in the Arabian Sea's OMZ', *Biogeosciences*, 9: 5095-109.

Rixen, Tim, Antje Baum, Birgit Gaye, and Birgit Nagel. 2014. 'Seasonal and interannual variations in the nitrogen cycle in the Arabian Sea', *Biogeosciences*, 11: 5733-47.

Rixen, Tim, Greg Cowie, Birgit Gaye, Joaquim Goes, Helga do Rosário Gomes, Raleigh R Hood, Zouhair Lachkar, Henrike Schmidt, Joachim Segschneider, and Arvind Singh. 2020. 'Reviews and syntheses: Present, past, and future of the oxygen minimum zone in the northern Indian Ocean', *Biogeosciences*, 17: 6051-80.

Rixen, Tim, Birgit Gaye, and Kay-Christian Emeis. 2019a. 'The monsoon, carbon fluxes, and the organic carbon pump in the northern Indian Ocean', *Progress in Oceanography*, 175: 24-39.

Rixen, Tim, Birgit Gaye, Kay-Christian Emeis, and Venkitasubramani Ramaswamy. 2019b. 'The ballast effect of lithogenic matter and its influences on the carbon fluxes in the Indian Ocean', *Biogeosciences*, 16: 485-503.

Rixen, Tim, and Venugopalan Ittekkot. 2005. 'Nitrogen deficits in the Arabian Sea, implications from a three component mixing analysis', *Deep Sea Research Part II: Topical Studies in Oceanography*, 52: 1879-91.

Sarma, V. V. S. S., A. Lenton, R. M. Law, N. Metzl, P. K. Patra, S. Doney, I. D. Lima, E. Dlugokencky, M. Ramonet, and V. Valsala. 2013. 'Sea-air CO2 fluxes in the Indian Ocean between 1990 and 2009', *Biogeosciences*, 10: 7035-52.

Sarma, VVSS, TVS Udaya Bhaskar, J Pavan Kumar, and Kunal Chakraborty. 2020. 'Potential mechanisms responsible for occurrence of core oxygen minimum zone in the north-eastern Arabian Sea', *Deep Sea Research Part I: Oceanographic Research Papers*, 165: 103393.

Sarma, VVSS, L Jagadeesan, HB Dalabehera, DN Rao, GS Kumar, DS Durgadevi, K Yadav, S Behera, and MMR Priya. 2018. 'Role of eddies on intensity of oxygen minimum zone in the Bay of Bengal', *Continental Shelf Research*, 168: 48-53.

Sarma, VVSS, MS Krishna, YS Paul, and VSN Murty. 2015a. 'Observed changes in ocean acidity and carbon dioxide exchange in the coastal Bay of Bengal–a link to air pollution', *Tellus B: Chemical and Physical Meteorology*, 67: 24638.

Sarma, VVSS, MS Krishna, VD Rao, R Viswanadham, NA Kumar, TR Kumari, L Gawade, S Ghatkar, and A Tari. 2012. 'Sources and sinks of CO2 in the west coast of Bay of Bengal', *Tellus B: Chemical and Physical Meteorology*, 64: 10961.

Sarma, VVSS, MS Krishna, TNR Srinivas, VR Kumari, K Yadav, and MD Kumar. 2021. 'Elevated acidification rates due to deposition of atmospheric pollutants in the coastal Bay of Bengal', *Geophysical Research Letters*, 48: e2021GL095159.

Sarma, VVSS, JS Patil, D Shankar, and AC Anil. 2019. 'Shallow convective mixing promotes massive Noctiluca scintillans bloom in the northeastern Arabian Sea', *Marine Pollution Bulletin*, 138: 428-36.

Sarma, VVSS, YS Paul, DG Vani, and VSN Murty. 2015. 'Impact of river discharge on the coastal water pH and pCO2 levels during the Indian Ocean Dipole (IOD) years in the western Bay of Bengal', *Continental Shelf Research*, 107: 132-40.

Sarma, VVSS, and TVS Udaya Bhaskar. 2018. 'Ventilation of oxygen to oxygen minimum zone due to anticyclonic eddies in the Bay of Bengal', *Journal of Geophysical Research: Biogeosciences*, 123: 2145-53.

Sathyendranath, Shubha, Venetia Stuart, Anitha Nair, Kenji Oka, Toru Nakane, Heather Bouman, Marie-Hélène Forget, Heidi Maass, and Trevor Platt. 2009. 'Carbon-to-chlorophyll ratio and growth rate of phytoplankton in the sea', *Marine Ecology Progress Series*, 383: 73-84.

Schmidt, Henrike, Rena Czeschel, and Martin Visbeck. 2020. 'Seasonal variability of the circulation in the Arabian Sea at intermediate depth and its link to the Oxygen Minimum Zone', *Ocean Science Discussions*.

Schmidt, Henrike, Julia Getzlaff, Ulrike Löptien, and Andreas Oschlies. 2021. 'Causes of uncertainties in the representation of the Arabian Sea oxygen minimum zone in CMIP5 models', *Ocean Science Discussions*: 1-32.

Schmidtko, Sunke, Lothar Stramma, and Martin Visbeck. 2017. 'Decline in global oceanic oxygen content during the past five decades', *Nature*, 542: 335-39.

Schunck, Harald, Gaute Lavik, Dhwani K Desai, Tobias Großkopf, Tim Kalvelage, Carolin R Löscher, Aurélien Paulmier, Sergio Contreras, Herbert Siegel, and Moritz Holtappels. 2013. 'Giant hydrogen sulfide plume in the oxygen minimum zone off Peru supports chemolithoautotrophy', *PloS ONE*, 8: e68661.

Schwartz, Matthew C, Clare Woulds, and Gregory L Cowie. 2009. 'Sedimentary denitrification rates across the Arabian Sea oxygen minimum zone', *Deep Sea Research Part II: Topical Studies in Oceanography*, 56: 324-32.

Seiwell, Harry Richard. 1937. *The minimum oxygen concentration in the western basin of the North Atlantic* (Massachusetts Institute of Technology).

SenGupta, R., and S. W. A. Naqvi. 1984. 'Chemical oceanography of the Indian Ocean, north of the equator', *Deep Sea Research Part A. Oceanographic Research Papers*, 31: 671-706.

Sewell, R. B. S. . 1934. 'The John Murray Expedition to the Arabian Sea', *Nature*, 133: 669-72.

SEWELL, RB SEYMOUR, and Louis Fage. 1948. 'Minimum oxygen layer in the ocean', *Nature*, 162: 949-51.

Shah, Chinmay, AK Sudheer, and Ravi Bhushan. 2018. 'Distribution of dissolved organic carbon in the Bay of Bengal: Influence of sediment discharge, fresh water flux, and productivity', *Marine Chemistry*, 203: 91-101.

Somasundar, K, A Rajendran, M Dileep Kumar, and R Sen Gupta. 1990. 'Carbon and nitrogen budgets of the Arabian Sea', *Marine Chemistry*, 30: 363-77.

Somes, Christopher J, Andreas Oschlies, and A Schmittner. 2013. 'Isotopic constraints on the pre-industrial oceanic nitrogen budget', *Biogeosciences*, 10: 5889-910.

Sredivi, B., and V. V. S. S. Sarma (2022) 'Enhanced Atmospheric pollutants strengthened winter convective mixing and phytoplankton blooms in the northern Arabian Sea', *Journal of Geophysical Research, Biogeosciences,* 127, e2021JG006527.

Sreeush, Mohanan Geethalekshmi, Saran Rajendran, Vinu Valsala, Sreenivas Pentakota, KVSR Prasad, and Raghu Murtugudde. 2019. 'Variability, trend and controlling factors of Ocean acidification over Western Arabian Sea upwelling region', *Marine Chemistry*, 209: 14-24.

Sreeush, Mohanan Geethalekshmi, Vinu Valsala, Sreenivas Pentakota, Koneru Venkata Siva Rama Prasad, and Raghu Murtugudde. 2018. 'Biological production in the Indian Ocean upwelling zones–Part 1: refined estimation via the use of a variable compensation depth in ocean carbon models', *Biogeosciences*, 15: 1895-918.

Sreeush, Mohanan Geethalekshmi, Vinu Valsala, Halder Santanu, Sreenivas Pentakota, KVSR Prasad, CV Naidu, and Raghu Murtugudde. 2020. 'Biological production in the Indian Ocean upwelling zones-Part 2: Data based estimates of variable compensation depth for ocean carbon models via cyclo-stationary Bayesian Inversion', *Deep Sea Research Part II: Topical Studies in Oceanography*, 179: 104619.

Sridevi, B, and VVSS Sarma. 2021. 'Role of river discharge and warming on ocean acidification and pCO2 levels in the Bay of Bengal', *Tellus B: Chemical and Physical Meteorology*, 73: 1-20.

Stramma, L., G. C. Johnson, J. Sprintall, and V. Mohrholz. 2008. 'Expanding oxygen-minimum zones in the tropical oceans,' *Science*, 320: 655-58.

Stramma, L., S. Schmidtko, L. A. Levin, and G. C. Johnson. 2010. 'Ocean oxygen minima expansions and their biological impacts', *Deep-Sea Research, Part I*, 57: 587-95.

Strutton, P. G., V. J. Coles, R. R. Hood, R. J. Matear, M. J. McPhaden, and H. E. Phillips. 2015. 'Biogeochemical variability in the central equatorial Indian Ocean during the monsoon transition', *Biogeosciences*, 12: 2367-82.

Subha Anand, S , R Rengarajan, Damodar Shenoy, Mangesh Gauns, and SWA Naqvi. 2018b. 'POC export fluxes in the Arabian Sea and the Bay of Bengal: A simultaneous 234Th/238U and 210Po/210Pb study', *Marine Chemistry*, 198: 70-87.

Subha Anand, S, R Rengarajan, and VVSS Sarma. 2018a. '234Th-based carbon export flux along the Indian GEOTRACES GI02 section in the Arabian Sea and the Indian Ocean', *Global Biogeochemical Cycles*, 32: 417-36.

Subha Anand, S, R Rengarajan, VVSS Sarma, AK Sudheer, R Bhushan, and SK Singh. 2017. 'Spatial variability of upper ocean POC export in the B ay of B engal and the I ndian O cean determined using particle-reactive 234 T h', *Journal of Geophysical Research: Oceans*, 122: 3753-70.

Sudheesh, V, GVM Gupta, KV Sudharma, H Naik, DM Shenoy, M Sudhakar, and SWA Naqvi. 2016. 'Upwelling intensity modulates N2O concentrations over the western I ndian shelf', *Journal of Geophysical Research: Oceans*, 121: 8551-65.

Sverdrup, H. U. , M. W. Johnson, and R. H. Fleming. 1942. *The Oceans: Their Physics, Chemistry and General Biology* (Prentice-Hall: Englewood Cliffs, N.J.).

Sverdrup, HU. 1938. 'On the explanation of the oxygen minima and maxima in the oceans', *ICES Journal of Marine Science*, 13: 163-72.

Swallow, J. . 1984. 'Some aspects of the physical oceanography of the Indian Ocean', *Deep Sea Research*, 31: 639-50.

Takahashi, T., and et al. 2009. 'Climatological mean and decadal change in surface ocean pCO2, and net sea-air CO2 flux over the global ocean', *Deep-Sea Rearch, part II*, 56: 554-77.

Takahashi, T., S.C. Sutherland, D. Chipman, J. G. Goddard, C. Ho, T. Newberger, C. Sweeney, and D. R. Munro. 2014. 'Climatological distributions of pH, pCO2, total CO2, alkalinity, and CaCO3 saturationh in the global surface ocean, and temporal changes at selected locations', *Marine Chemistry*, 164: 95-125.

Takahashi, T., S.C. Sutherland, C. Sweeney, A. Poisson, N. Metzl, B. Tilbrook, N. Bates, R. Wanninkhof, R.A. Feely, C. Sabine, J. Olafsson, and Y. Nojiri. 2002. 'Global sea-air CO_2 flux based on climatological surface ocean pCO_2, and seasonal biological and temperature effects', *Deep-Sea Research Part II*, 49: 1601-23.

Talley, Lynne D, Gregory C Johnson, Sarah Purkey, Richard A Feely, and Rik Wanninkhof. 2017. "Global Ocean Ship-based Hydrographic Investigations Program (GO-SHIP) provides key climate-relevant deep ocean observations, US CLIVAR Variations, 15." In.

Tarique, Mohd, Waliur Rahaman, AA Fousiya, N Lathika, Meloth Thamban, Hema Achyuthan, and Sambuddha Misra. 2021. 'Surface pH Record (1990–2013) of the Arabian Sea From Boron Isotopes of Lakshadweep Corals—Trend, Variability, and Control', *Journal of Geophysical Research: Biogeosciences*, 126: e2020JG006122.

Tchernia, Paul. 1980. 'Descriptive regional oceanography'.

Thushara, Venugopal, Puthenveettil Narayana Menon Vinayachandran, Adrian J Matthews, Benjamin GM Webber, and Bastien Y Queste. 2019. 'Vertical distribution of chlorophyll in dynamically distinct regions of the southern Bay of Bengal', *Biogeosciences*, 16: 1447-68.

Udaya Bhaskar, TVS, VVSS Sarma, and J Pavan Kumar. 2021. 'Potential mechanisms responsible for spatial variability in intensity and thickness of oxygen minimum zone in the Bay of Bengal', *Journal of Geophysical Research: Biogeosciences*, 126: e2021JG006341.

Vallivattathillam, Parvathi, Suresh Iyyappan, Matthieu Lengaigne, Christian Ethé, Jérôme Vialard, Marina Levy, Neetu Suresh, Olivier Aumont, Laure Resplandy, and Hema Naik. 2017. 'Positive Indian Ocean Dipole events prevent anoxia off the west coast of India', *Biogeosciences*, 14: 1541-59.

Valsala, V., S. Maksyutov, and R. Murtugudde. 2012. 'A window for carbon uptake in the southern subtropical Indian Ocean', *Geophysical Research Letters*, 39: L17605.

Valsala, Vinu. 2009. 'Different spreading of Somali and Arabian coastal upwelled waters in the northern Indian Ocean: A case study', *Journal of Oceanography*, 65: 803-16.

Valsala, Vinu, and Shamil Maksyutov. 2010. 'Simulation and assimilation of global ocean pCO2 and air–sea CO2 fluxes using ship observations of surface ocean pCO2 in a simplified biogeochemical offline model', *Tellus B: Chemical and Physical Meteorology*, 62: 821-40.

———. 2013. 'Interannual variability of the air–sea CO2 flux in the north Indian Ocean', *Ocean Dynamics*, 63: 165-78.

Valsala, Vinu, and Raghu Murtugudde. 2015. 'Mesoscale and intraseasonal air–sea CO2 exchanges in the western Arabian Sea during boreal summer', *Deep Sea Research Part I: Oceanographic Research Papers*, 103: 101-13.

Valsala, Vinu, MG Sreeush, and Kunal Chakraborty. 2020. 'The IOD impacts on the Indian Ocean Carbon cycle', *Journal of Geophysical Research: Oceans*, 125: e2020JC016485.

Valsala, Vinu, Mohanan Geethalekshmi Sreeush, M Anju, Pentakota Sreenivas, Yogesh K Tiwari, Kunal Chakraborty, and S Sijikumar. 2021. 'An observing system simulation experiment for Indian Ocean surface pCO2 measurements', *Progress in Oceanography*, 194: 102570.

Vaquer-Sunyer, Raquel, and Carlos M Duarte. 2008. 'Thresholds of hypoxia for marine biodiversity', *Proceedings of the National Academy of Sciences*, 105: 15452-57.

Vinayachandran, P. N. 2009. 'Impact of physical processes on chlorophyll distribution in the Bay of Bengal.' in J. D. Wiggert, R. R. Hood, S. W. A. Naqvi, K. H. Brink and S. L. Smith (eds.), *Indian Ocean Biogeochemical Processes and Ecological Variability* (American Geophysical Union: Washington D.C.).

Volk, T., and M. I. Hoffert. 1985. 'The carbon cycle and atmospheric CO2, natural variation archean to present', *In E.T. Sundquist, W.S. Broecker (Eds.), The Carbon Cycle and Atmospheric CO2: Natural Variations Archean to Present, Vol. Geophysical Monograph 32 (pp. 99-110). Washington: AGU.*

Waite, Anya M, Lars Stemmann, Lionel Guidi, Paulo HR Calil, Andrew Mc C Hogg, Ming Feng, Peter A Thompson, Marc Picheral, and Gaby Gorsky. 2016. 'The wineglass effect shapes particle export to the deep ocean in mesoscale eddies', *Geophysical Research Letters*, 43: 9791-800.

Weeks, Scarla J, Bronwen Currie, and Andrew Bakun. 2002. 'Massive emissions of toxic gas in the Atlantic', *Nature*, 415: 493-94.

Woods, John D. 1985. 'The world ocean circulation experiment', *Nature*, 314: 501-11.

Table 1: Definitions, thresholds, and impacts of different hypoxia thresholds from Hofmann et al 2011.

Terminology	Threshold for impacts to occur maybe in different units	Impacts	Indian Ocean Regions with oxygen minimums below threshold	References
Mild Hypoxia	107 µmol/kg, 109 µM, 3.5 mgO2/l, ~53 % saturation,	Sensitive species show avoidance reactions	Eastern and Central Indian Ocean south of 20S, Western Indian Ocean south of 10S	Cenr 2010
Hypoxia	61µmol/kg, 63µM, 2 mgO2/l, ~30 % saturation,	Fishes and the majority of higher organisms suffer from oxygen deficiency, ecosystem adapted to low oxygen conditions	Arabian Sea, Bay of Bengal	Ekau et al., 2010; Vaquer-Sunyer and Duarte 2008
Microbial hypoxia, suboxic, Severe hypoxia, typical OMZ definition.	22 µmol/kg, 22 µM, 0.71 mgO2/l, ~11 % saturation	Microbes start to experience the toxic effects of oxygen on anaerobic processes, only highly specialized species survive	Northern tropical Indian Ocean	Rixen et al., 2020, Diaz and Rosenburg (2008)
Functional anoxia	0.05 µM	Anaerobic microbial processes dominate, nitrite accumulation	Central and Eastern Arabian Sea.	Rixen et al., 2020, Morrison et al., 1999, Ulloa et al, 2012

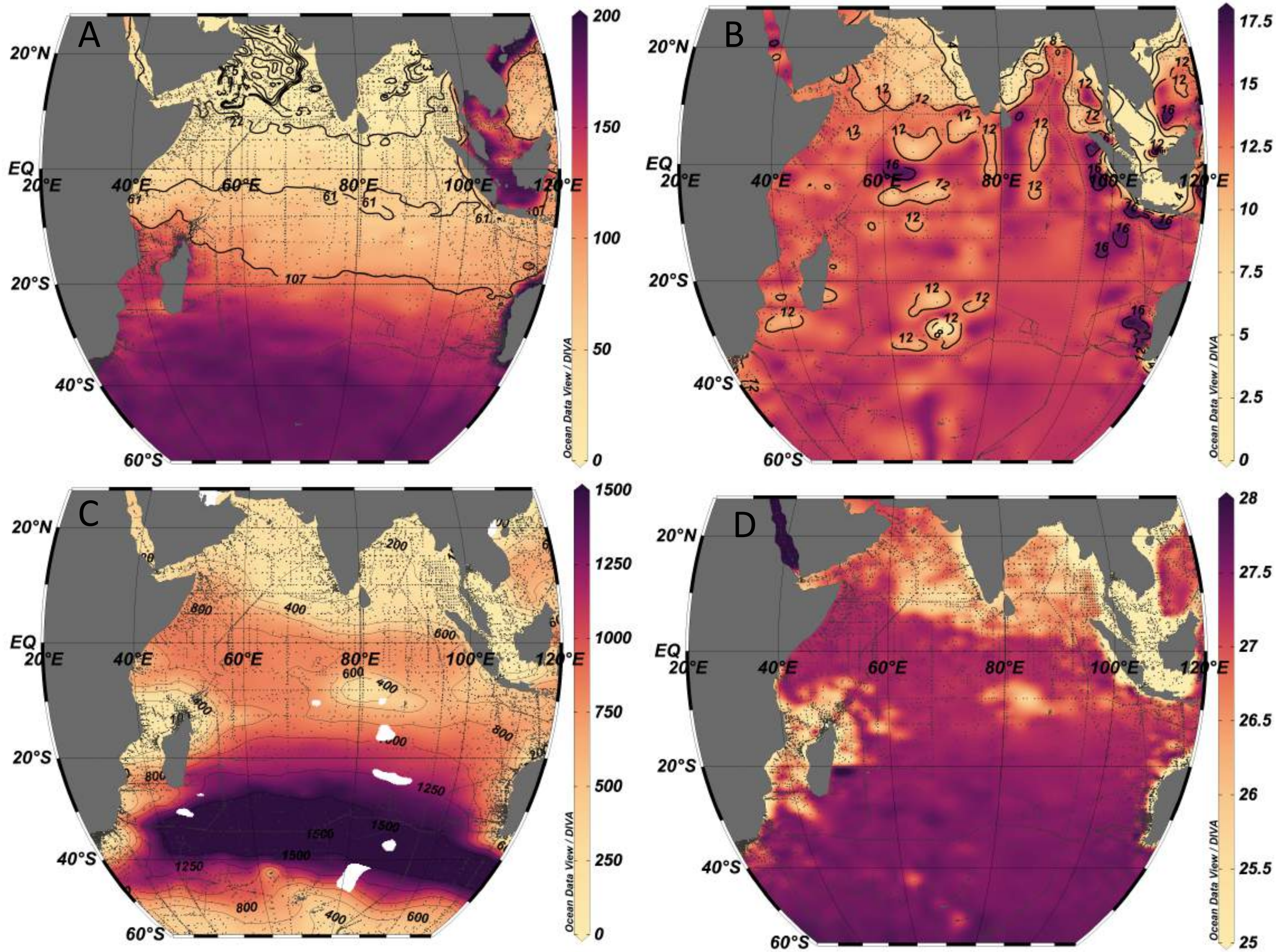

Figure 1: Spatial maps of the A) oxygen concentration (umol/kg) at the depth of the oxygen minimum, B) nitrate to phosphorus ratio at the depth of the oxygen minimum, C) the depth (m) of the oxygen minimum, D) the potential density anomaly (kg/m3) at the depth of the oxygen minimum.

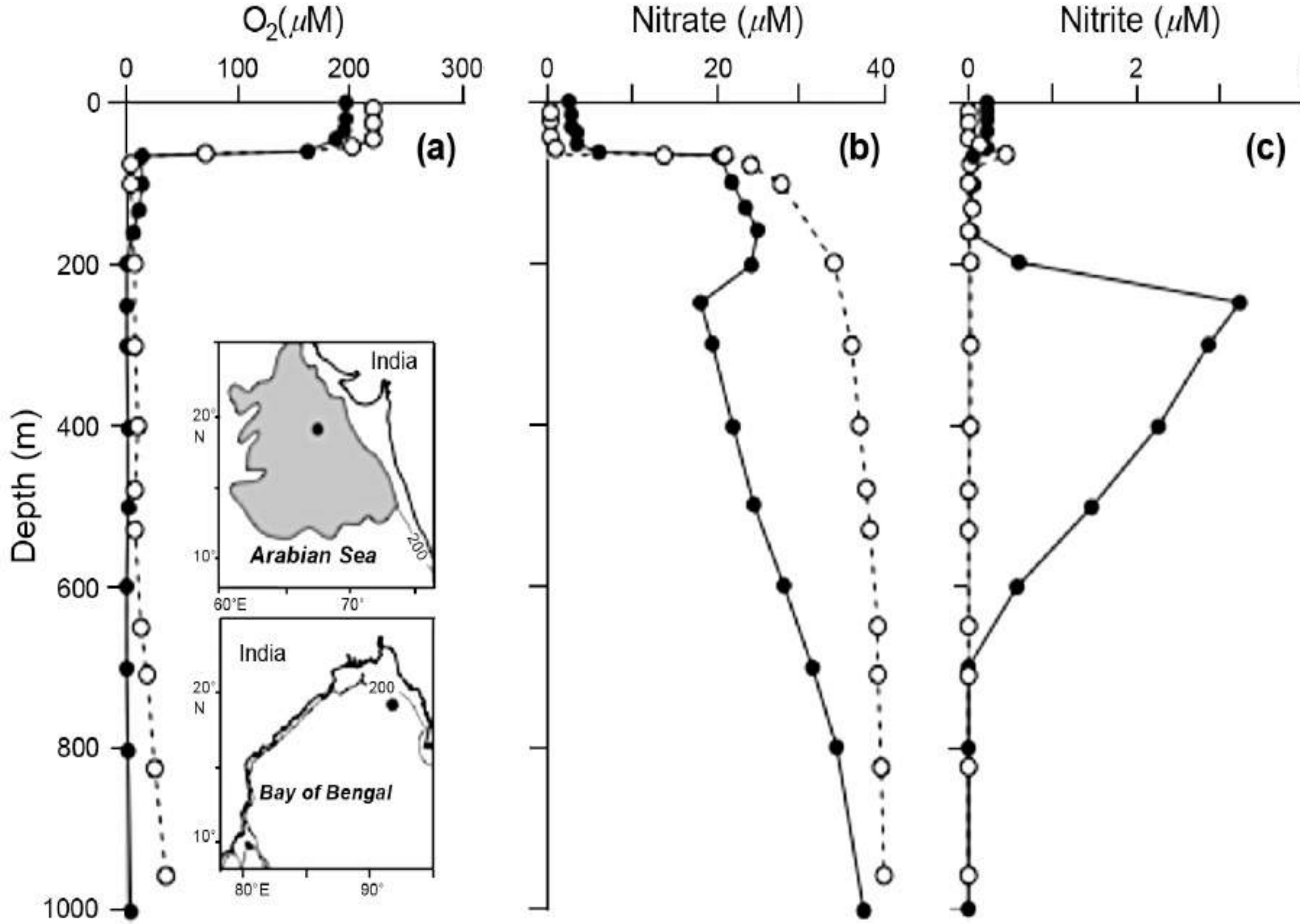

Figure 2: Comparison of vertical profiles of (a) oxygen, (b) nitrate and (c) nitrite in the Arabian Sea (filled circles) and Bay of Bengal (open circles). Station locations are shown in insets. The Arabian Sea inset also shows limit of the denitrification zone to the eastern-central basin. Figure reproduced from Naqvi et al. (2006).

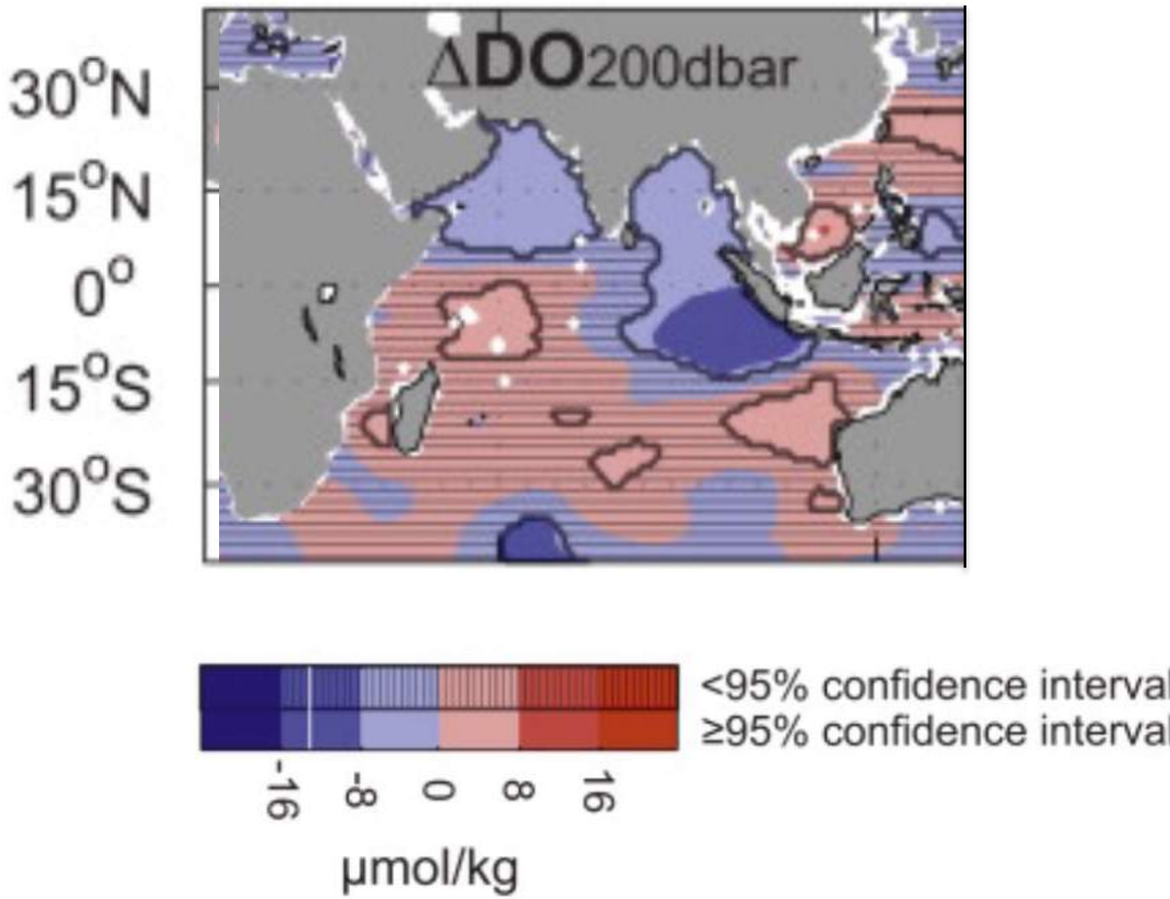

Figure 3: Changes in dissolved oxygen (DO) (μmol kg−1) at 200 dbar between 1960–1974 and 1990–2008 in the Indian Ocean. Increases (decreases) in DO are indicated in red (blue). Areas with differences below the 95% confidence interval are shaded by black horizontal lines. Figure modified from Stramma et al. (2010).

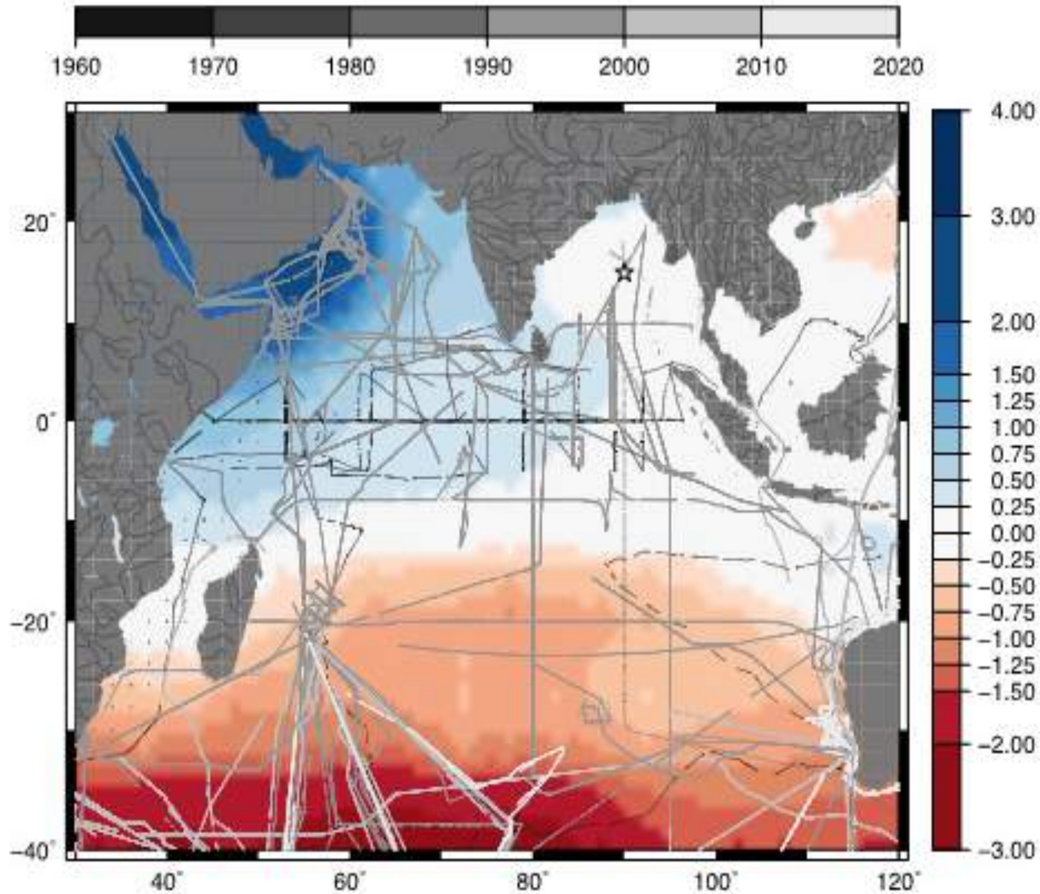

Figure 4: Annual CO_2 flux (mol C m^{-2} yr^{-1}) referenced to the year 2000 (Takahashi et al., 2009) over the Indian Ocean. Data points colored by year of collection (Takahashi & Sutherland, 2016) are overlaid as points. Major rivers are also delineated over the continents. The star in the central Bay of Bengal shows the location of a mooring that has been collecting continuous CO_2 and pH measurements since November, 2013. Figure and caption from Hood et al. (2019).

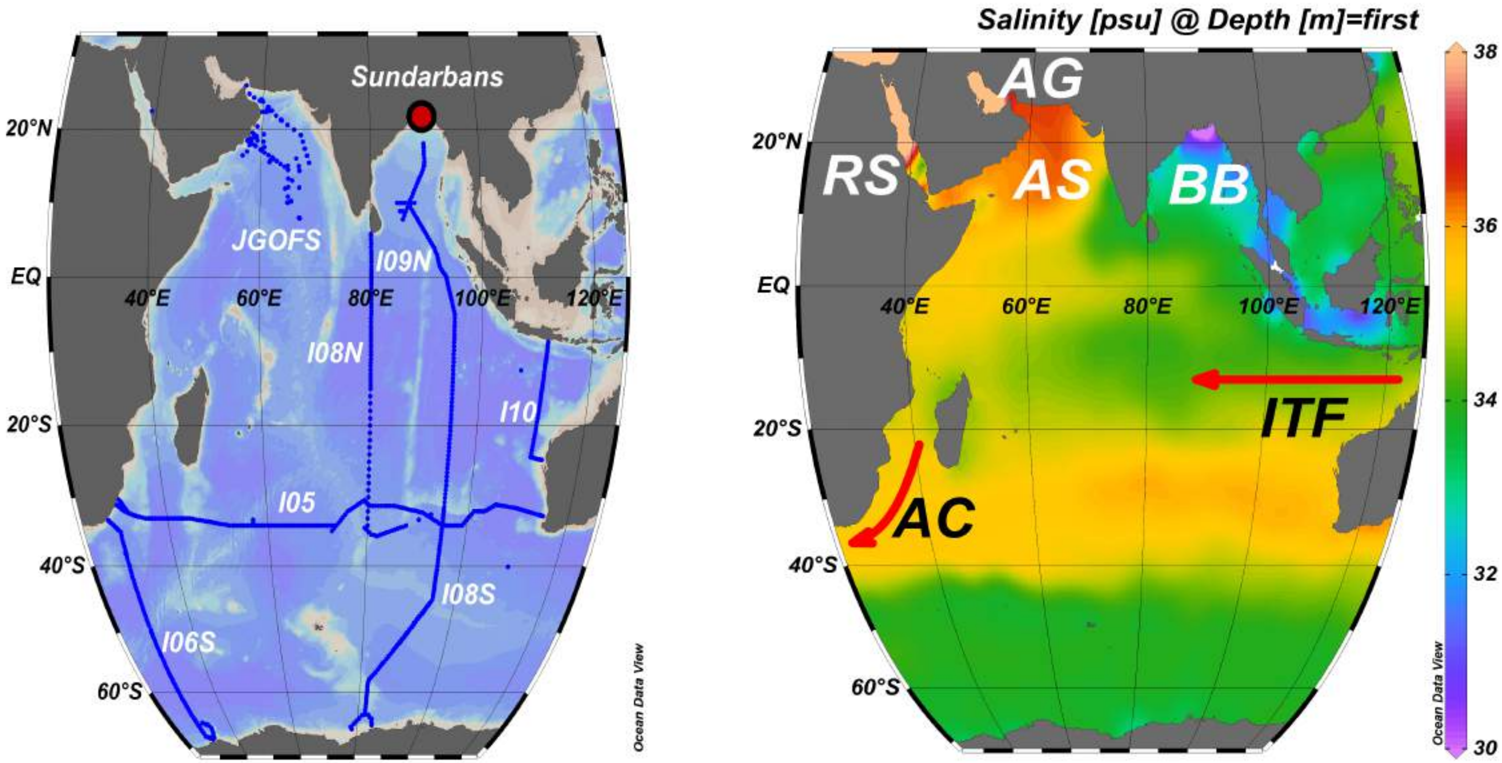

Figure 5: Map of the Indian Ocean showing oceanographic sections discussed (left) and gridded surface salinity (right) during austral summer (WOA), with transports associated with the Indonesian Throughflow (ITF) and Agulhas Current (AC) indicated. Relevant basins are labeled: Arabian Sea (AS); Bay of Bengal (BB); Red Sea (RS); Arabian Gulf (AG), also known as the Persian Gulf.

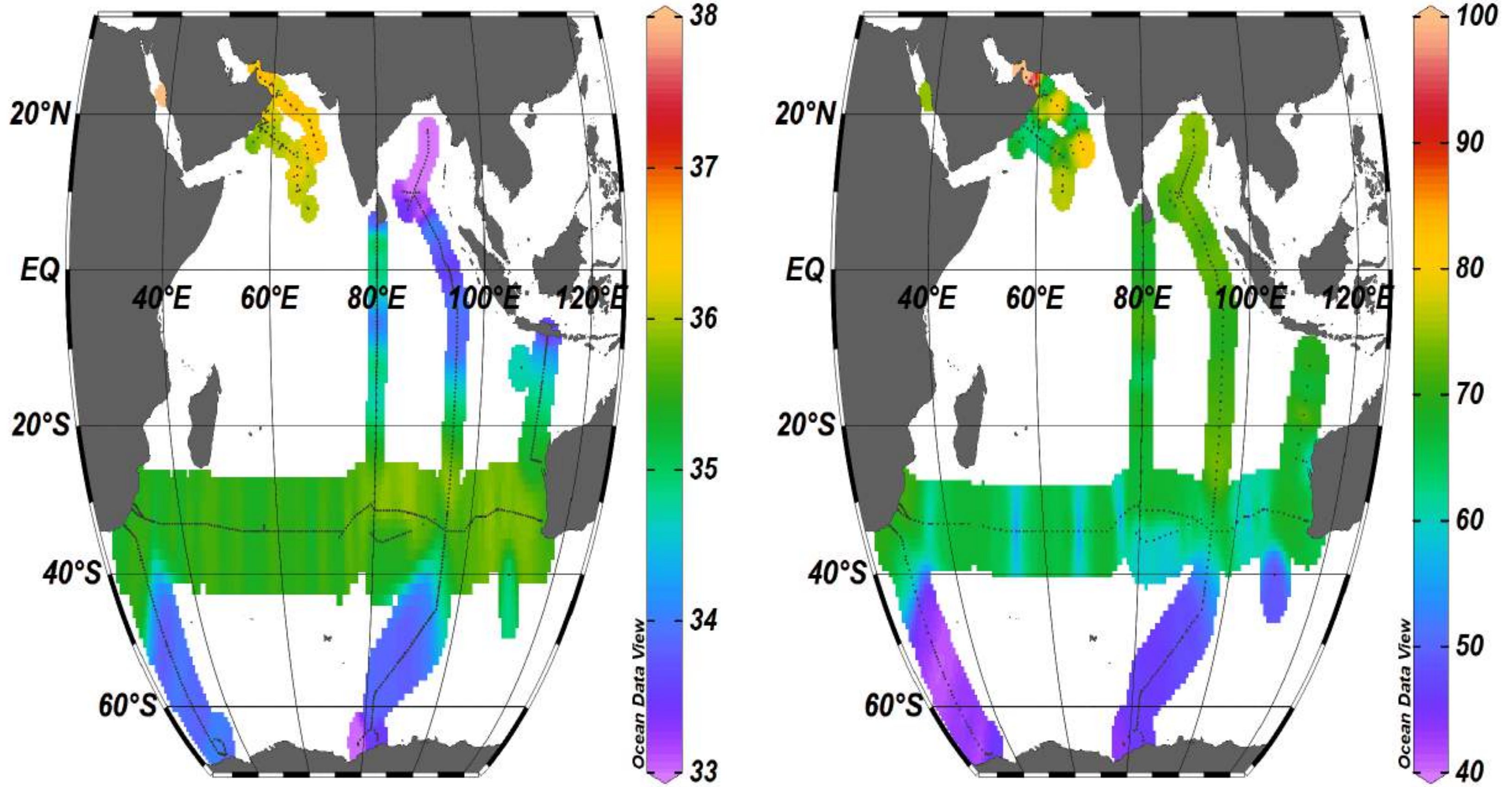

Figure 6: Surface distributions of salinity (left) and DOC (μmolC/kg; right) observed during cruises. Data from Hansell et al. (2021).

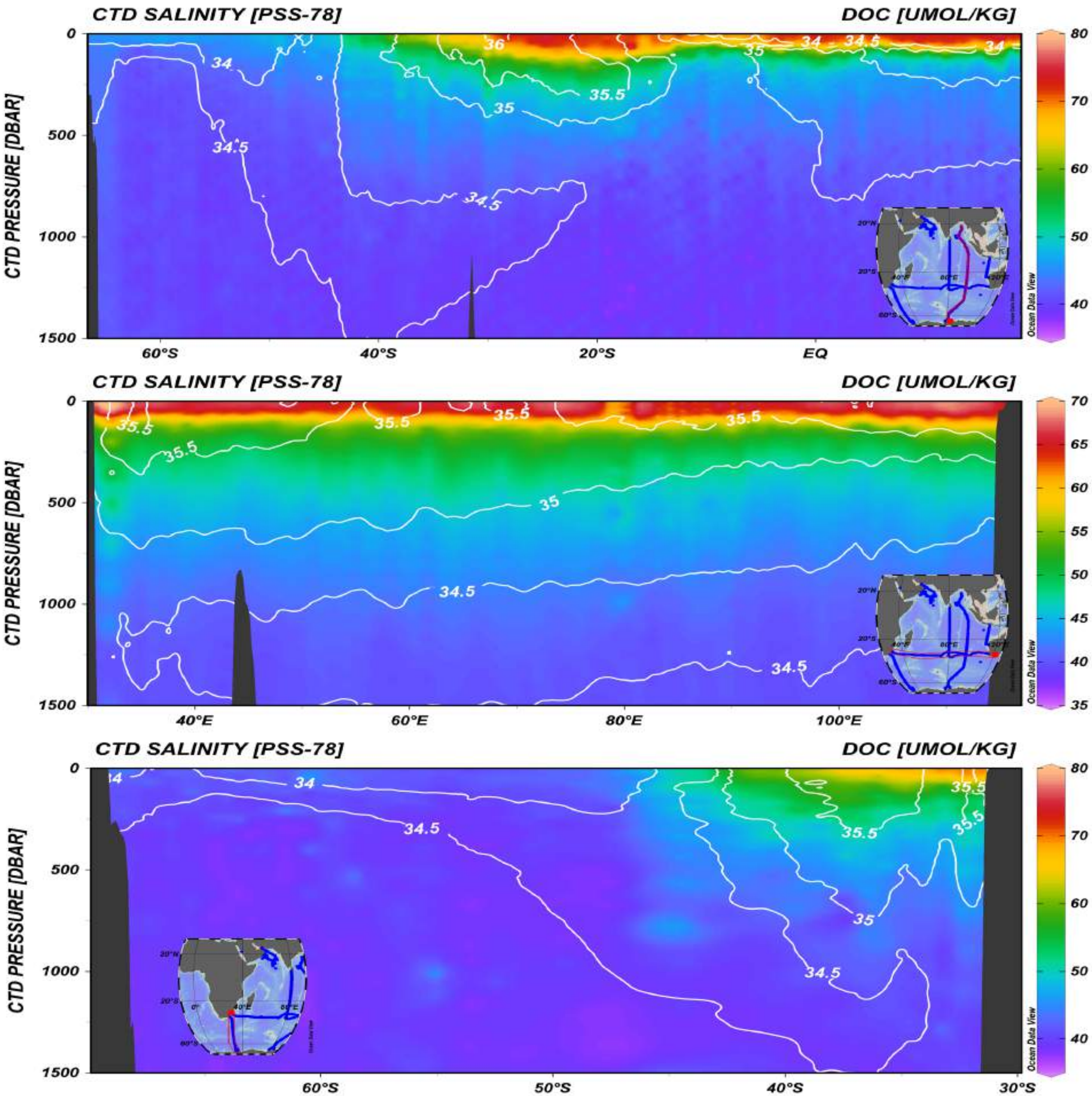

Figure 7: Upper 1500 m section plot of DOC (color; μmolC/kg) and salinity (contours) along I09N/I08S (top panel, occupied in 2016), I05 (middle panel, occupied in 2009) and I06S (bottom panel, occupied in 2019). Data from Hansell et al. (2021).

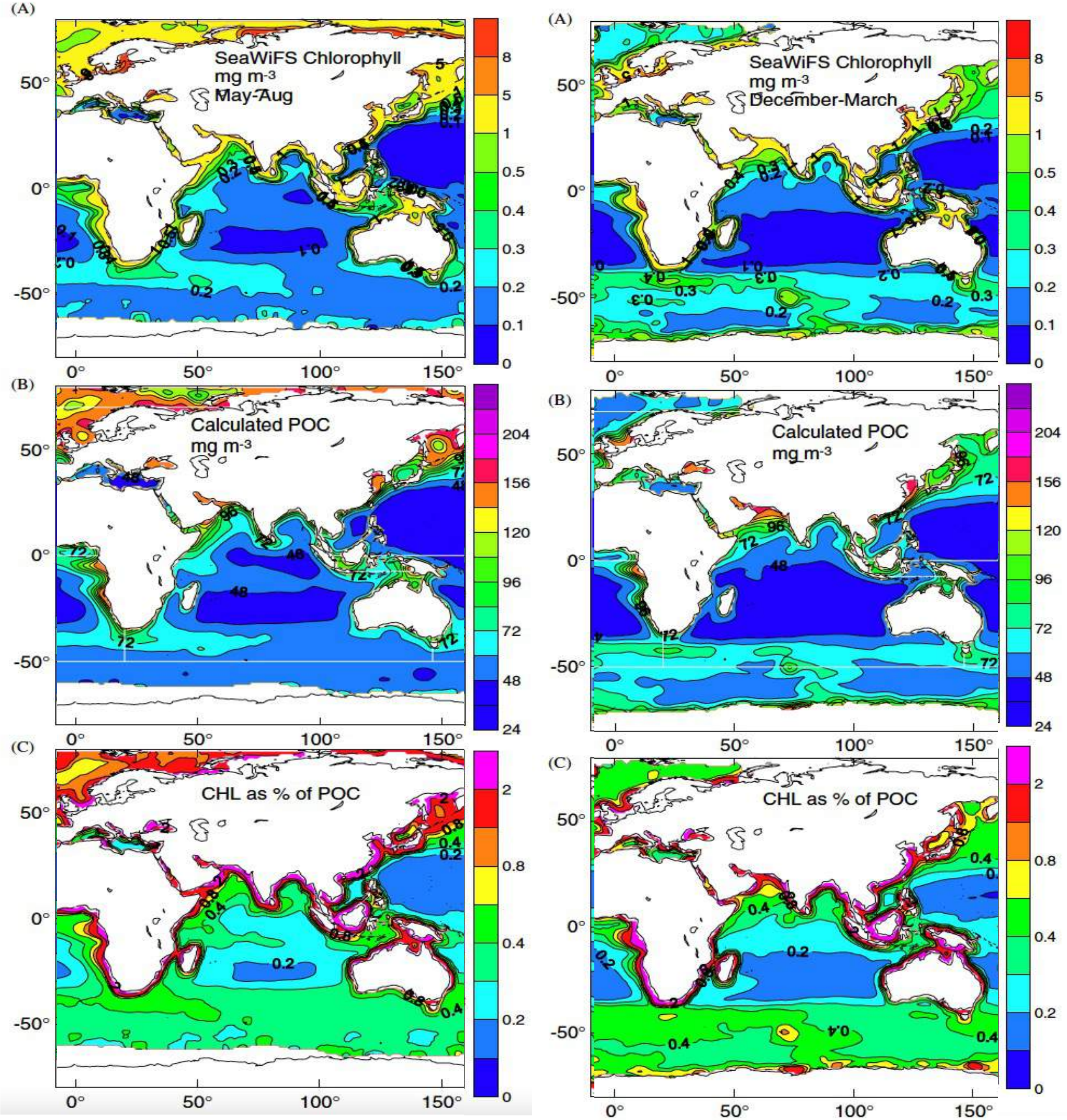

Figure 8: Distribution of: (A) SeaWiFS CHL (mg m^{-3}, level 3, reprocessing 4 data); (B) average POC (mgC m^{-3}) over one attenuation depth calculated from K_{490}:c_p:POC; (C) CHL as a % of POC for: (Left Panels) summer season (1997–2002, May–August, 20 months); (Right Panels) winter season (1997–2002, December–March, 20 months). White lines in (B) mark boundaries separating ocean basins as used by Behrenfeld and Falkowski (1997). Figure and caption modified from Gardner et al. (2006).

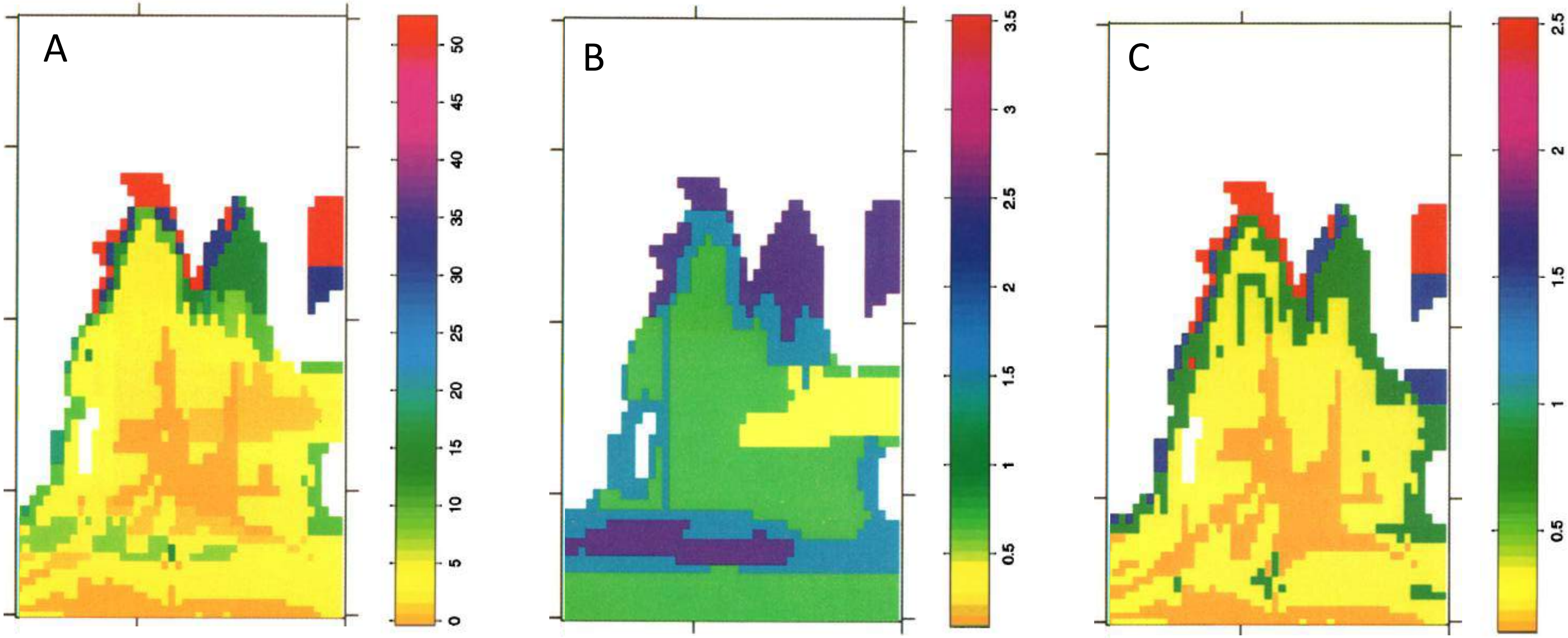

Figure 9: Estimated A) organic carbon burial rate (mmolC m^{-2} yr^{-1}); B) sediment accumulation rate (grams per square centimeter per thousand years); and C) seafloor distribution of organic carbon (weight percent). Figures and caption modified from Jahnke (1996).

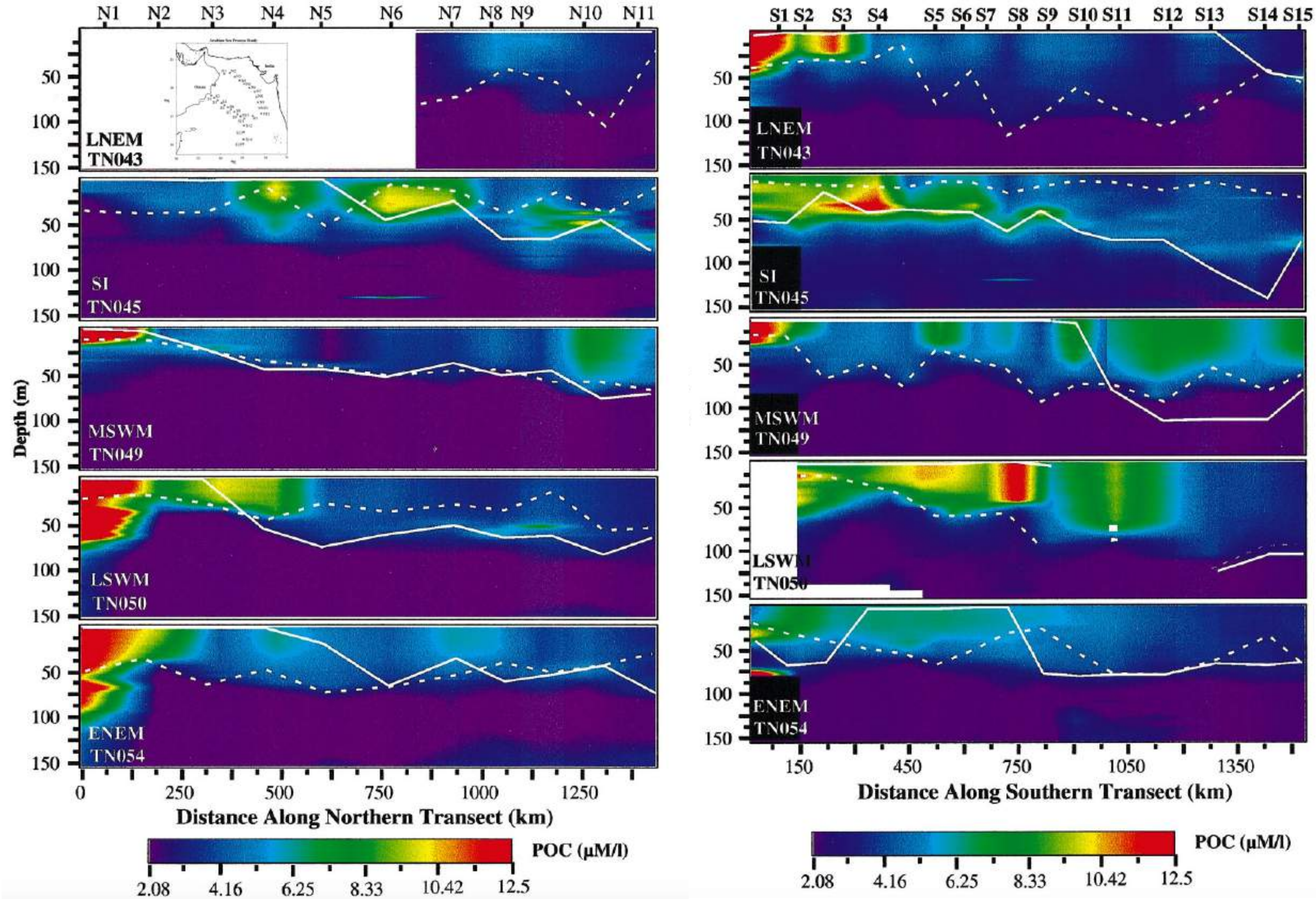

Figure 10: POC sections of the northern transect (left panels) and southern transect (right panels) for each cruise. Mean MLD [delta sigma = 0.03] (dotted line) and 0.5 µM/l nitrate isopleth (solid line) are shown for each cruise. The station locations are shown in the map inset in the upper left panel. Figures and caption modified from Gunderson et al. (1998).

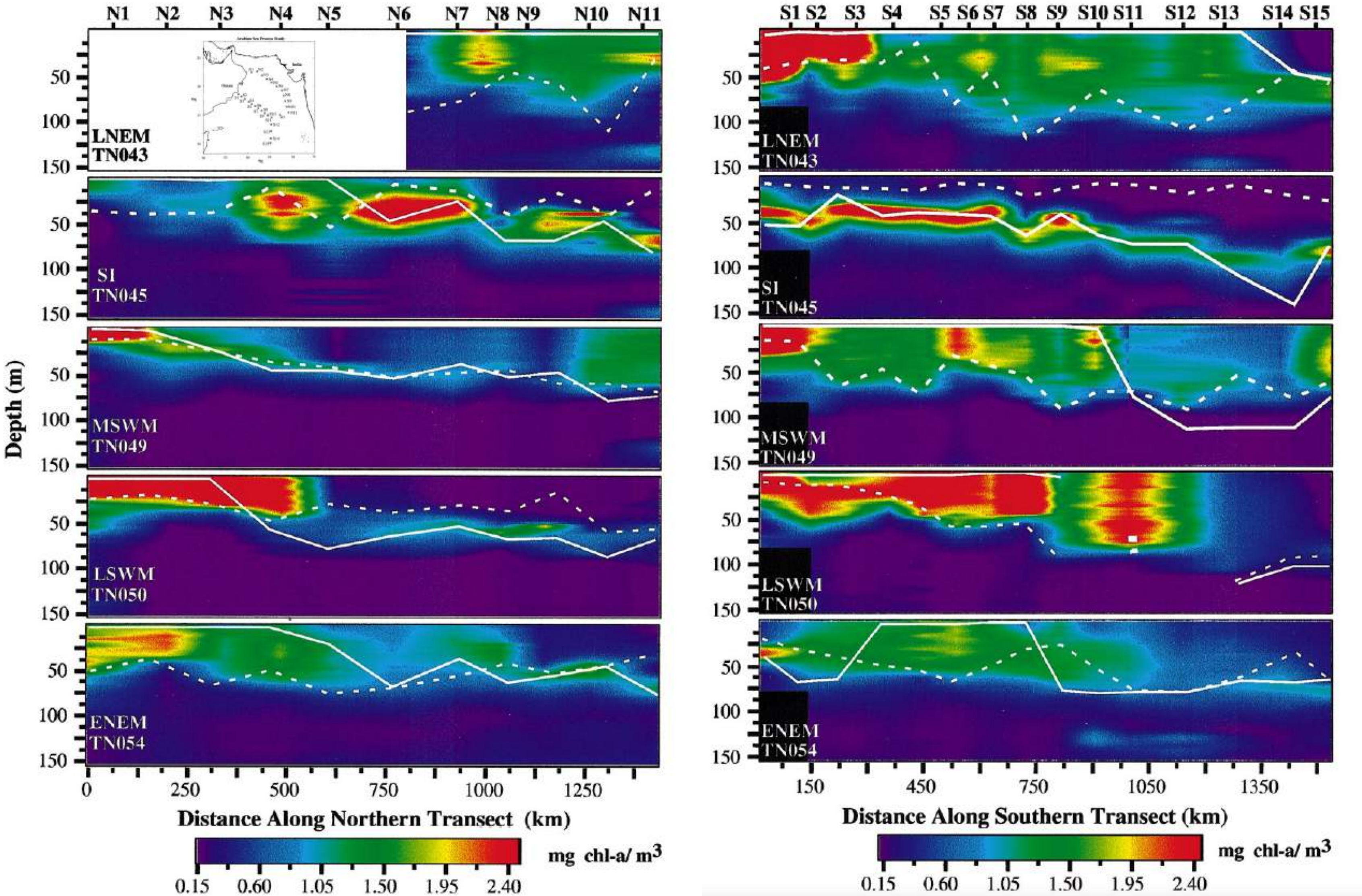

Figure 11: Chlorophyll sections of the northern transect (left panels) and southern transect (right panels) for each cruise. Mean MLD [delta sigma = 0.03] (dotted line) and 0.5 μM/l nitrate isopleth (solid line) are shown for each cruise. The station locations are shown in the map inset in the upper left panel. Figures and caption modified from Gunderson et al. (1998).

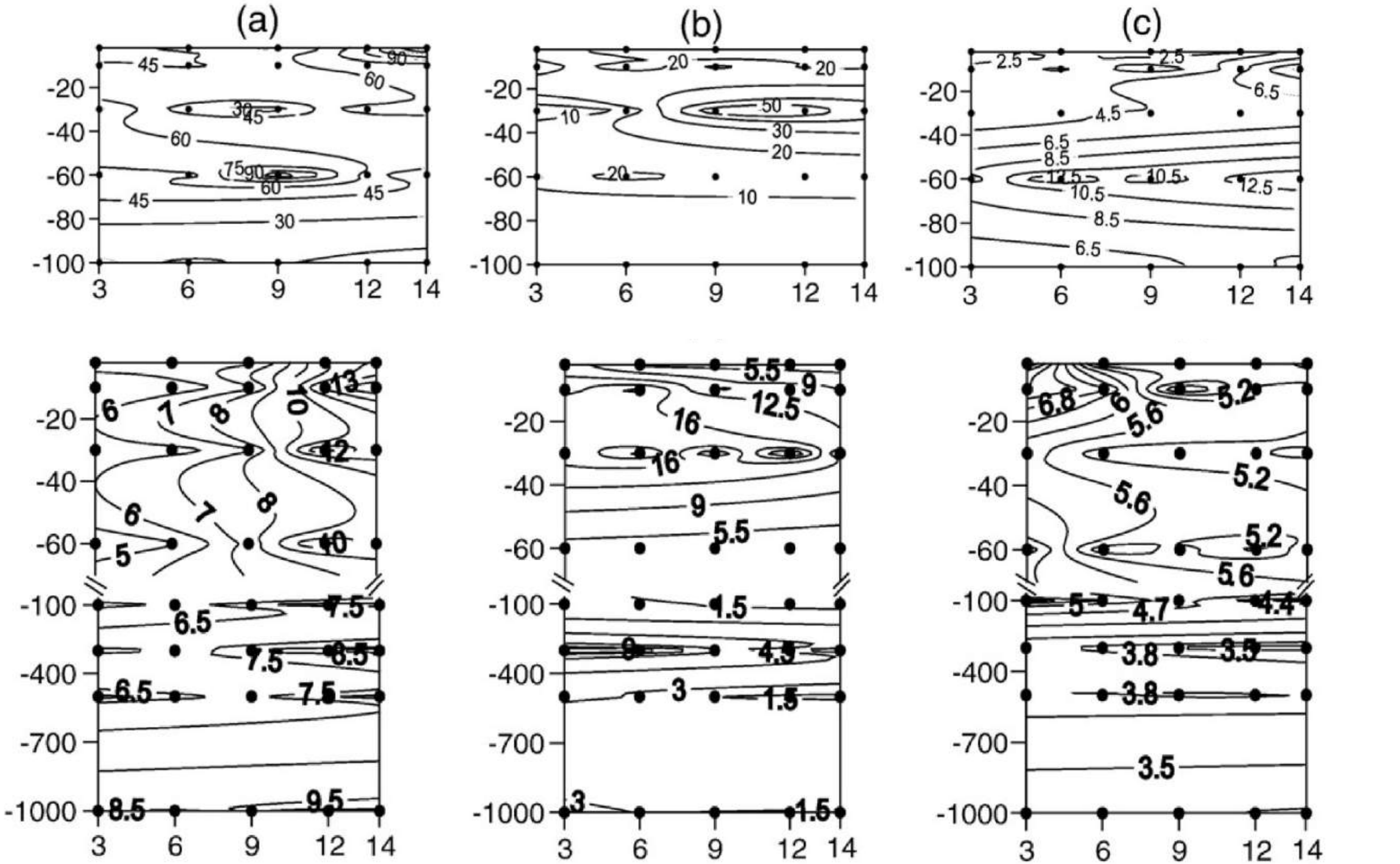

Figure 12: Distributions of chlorophyll a concentration (Chl a ng/l, top panels) and particulate organic carbon (POC µM C, bottom panels) in the central Bay of Bengal during (a) SWM, (b) FIM and (c) SPIM. Figure and caption modified from Fernandes et al. (2009).

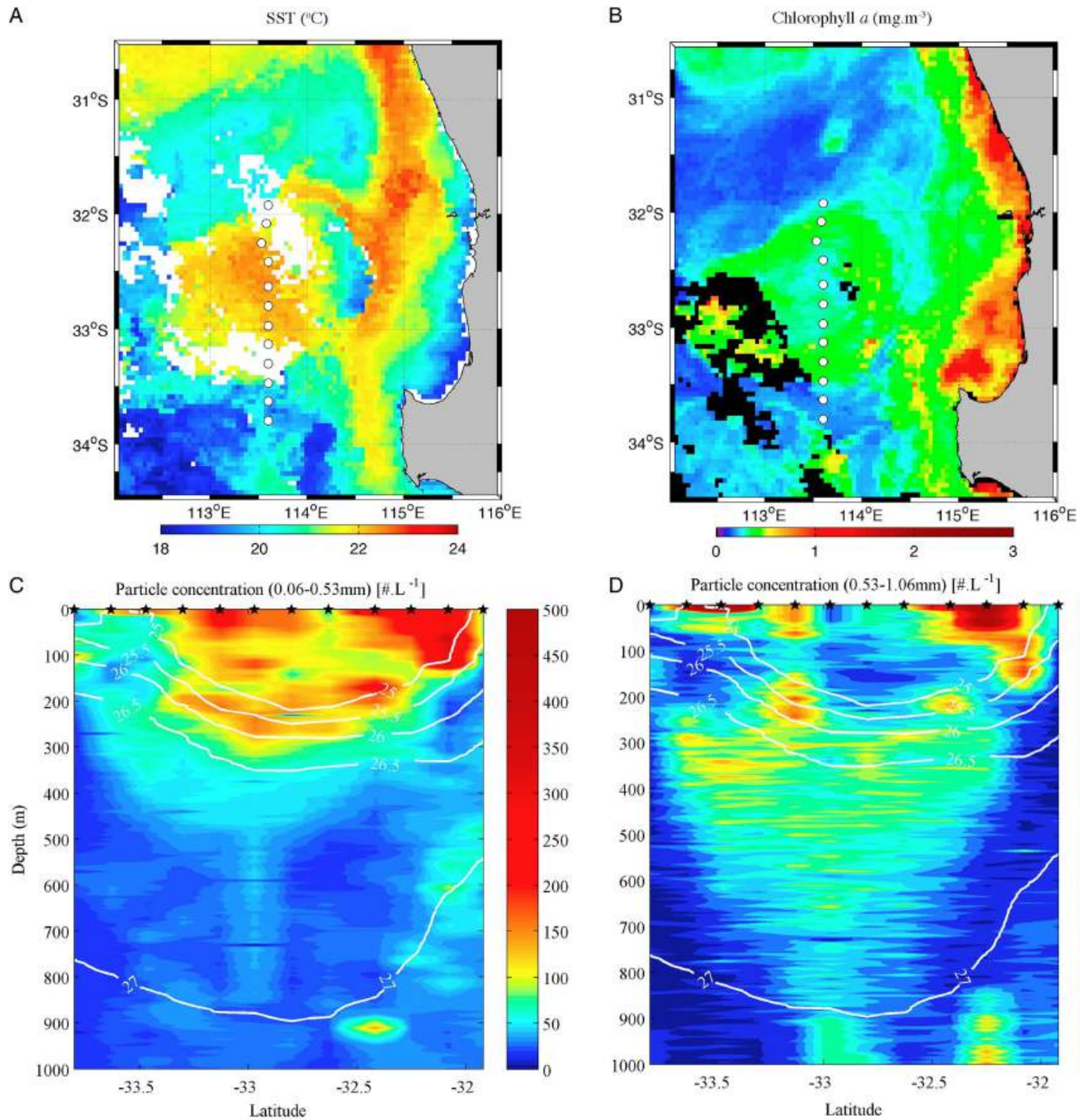

Figure 13: (a) Sea-surface temperature (°C) and (b) chlorophyll a (mg m^{-3}) derived from Moderate Resolution Imaging Spectroradiometer (MODIS) satellite, showing the mesoscale eddy in the Leeuwin Current (LC) off Australia. White circles indicate stations sampled. Spatial distributions of particles across the eddy: (c) Small (0.06–0.5 mm) and (d) large (0.5–1 mm) particles shown in color, with isopycnals contoured in white. Figures and caption modified from Waite et al. (2016).